

NASA Contract Report 166023

ANALYTICAL PROCEDURES FOR FLUTTER MODEL DEVELOPMENT  
AND CHECKOUT IN PREPARATION FOR WIND TUNNEL TESTING  
OF THE DAST ARW-1 WING

Samuel Pines

ANALYTICAL MECHANICS ASSOCIATES, INC.  
Hampton, Virginia 23666

CONTRACT NAS1-15593  
December 1982



National Aeronautics and  
Space Administration

**Langley Research Center**  
Hampton, Virginia 23665

### SUMMARY

This report describes the analytic procedures used to prepare for wind tunnel flutter testing of the DAST ARW-1 cantilevered wing model. The report contains a description of the methods used to:

- 1) Obtain an analytical realistic simulation of the structural, inertial and aerodynamic properties of the wing.
- 2) Obtain an analytical representation of the electro-servo actuator used for flutter suppression.
- 3) Obtain an open loop prediction of the flutter speed at a fixed Mach number (.897) vs. dynamic pressure.
- 4) Develop a procedure for calibrating the flutter model at different dynamic pressures and to check out the feed back flutter suppression law.
- 5) Obtain an analytical representation of a reduced state approximation to the full open loop simulation to be used in control system computer laboratory at the LaRC.

TABLE OF CONTENTS

<u>Section</u>	<u>Title</u>	<u>Page</u>
	SUMMARY . . . . .	i
	LIST OF FIGURES . . . . .	iii
	LIST OF TABLES . . . . .	iv
	INTRODUCTION . . . . .	1
I	DESCRIPTION OF THE WING FLUTTER MODEL . . . . .	3
II	STRUCTURAL INFLUENCE COEFFICIENT . . . . .	5
III	MASS DATA . . . . .	9
IV	FREQUENCIES AND MODES . . . . .	10
V	THE SOUSSA PROGRAM AND THE PADE APPROXIMANTS . . . . .	11
VI	THE HYDRAULIC ACTUATOR AND THE HYDRO-ELECTRO VALVE SYSTEM . . . . .	17
VII	EQUATIONS OF MOTION . . . . .	19
VIII	OPEN LOOP FLUTTER ANALYSIS . . . . .	23
IX	FLUTTER SUPPRESSION UTILIZING THE COMPLETE MODEL . . . . .	24
X	TESTING AND CALIBRATION OF THE ACTUATOR FEED BACK LAW . . . . .	30
XI	FLUTTER SUPPRESSION UTILIZING A REDUCED STATE . . . . .	35
	REFERENCES . . . . .	80

## LIST OF FIGURES

<u>Figure No.</u>	<u>Title</u>	<u>Page</u>
1	Wing planform of DAST-ARW1 . . . . .	37
2	Sketch of SPAR cross section along elastic axis . . . . .	38
3	Structural stiffness . . . . .	39
4	Coordinate system . . . . .	40
5	Dynamical coordinate system . . . . .	41
6	SPAR model . . . . .	42
7	Grid points constrained in reduced SPAR model . . . . .	43
8	Measured nodal patterns and frequencies . . . . .	44
9a	Mode 1 (5 hz) . . . . .	45
9b	Mode 2 (19 hz) . . . . .	46
9c	Mode 3 (26 hz) . . . . .	47
9d	Mode 4 (44 hz) . . . . .	48
10	Mode 5 (60 hz) . . . . .	49
11	Mode 6 (74 hz) . . . . .	50
12	First four normal modes of reduced dynamical system at zero airspeed . . . . .	51
13	Actuator . . . . .	52
14	Open loop eigenvalues of flexible modes as a function of dynamic pressure . . . . .	53
15	Dynamic-pressure root locus at $M = 0.90$ (system off), (Ref. 1) . . . . .	54
16	Damping and frequency versus dynamic pressure (system off) . . . . .	55

LIST OF TABLES

<u>Table No.</u>	<u>Title</u>	<u>Page</u>
1	SPAR Geometry Details . . . . .	38
2	Matrix of Influence Coefficients . . . . .	56
3	Combined Beam and Plate Element Mass Properties . . .	58
4	Concentrated Mass Properties in X-Y Coordinate System. . . . .	59
5	Mass Matrix . . . . .	60
6	Comparison of Vibration Modes . . . . .	62
7	$H_1$ Matrix . . . . .	63
8	$H_2$ Matrix . . . . .	65
9	$H_3$ Matrix . . . . .	67
10	Elements of Diagonal Matrix $F_p$ . . . . .	69
11	$Q_R(m,o)$ Steady State Lift and Moment . . . . .	70
12	Damping Coefficient Matrix $D_W$ . . . . .	72
13	Real Transformation Matrix $(Y)_{51x51}$ . . . . .	74
14	Real Jordan Eigenvalue Matrix $(\Omega)_{51x51}$ . . . . .	79

## INTRODUCTION

Real time, feedback control for flutter suppression is under serious study and consideration for aircraft (Refs. 1,2,3,4). The modal method (Refs. 5,6) is well suited for application in flutter suppression since the onset of flutter may be adequately described as a linear system instability (Ref. 7). Previous analyses of the problem have employed generalized coordinates, based on zero airspeed vibration modes or other fixed wing deformation shapes, from which generalized aerodynamic forces have been computed (Refs. 1,2,4). The contribution of this report is that physical coordinates of bending and torsion of the wing structure are directly employed, and that constant influence coefficient matrices are used to describe the structural, inertial and aerodynamic forces over a wide range of Mach numbers and airspeed. The aerodynamic influence coefficients were obtained through a modification of the SOUSSA digital program (Refs. 8,9) generated with the assistance of Prof. L. Morino of Boston University, Dr. E. C. Yates and H. Cunningham of NASA/LaRC. In contrast, the aerodynamic coefficients used in Ref. 1,12 were obtained using a doublet lattice method (Ref. 10). The method of Pade' approximants (Refs. 7,11,12,13) was applied to derive the aerodynamic influence coefficients in the real time domain. The structural influence coefficients were obtained through the use of the SPAR computer program at NASA/LaRC. The structural and geometric data of the DAST ARW-1 Wing, at 111 grid points, was supplied by Mr. R. Doggett of NASA/LaRC.

An application of the use of physical coordinates in the real time domain for flutter suppression is contained in Ref. 14. The major improvement contained in this study is the application of a better state of the art of the unsteady aerodynamic model (Refs. 8,9).

An earlier study (Ref. 15) for flutter suppression of the DAST ARW-1 wing was carried out for NASA LaRC. In order to prepare the use of the wing model in a flutter suppression wind tunnel test, it was necessary to develop a model of the control system actuator and integrate the effect of the hydraulic actuator constraint and the electrical valve

---

This study was funded by NASA Langley Research Center under Contract NAS1-15593.

response of the feed back control loop into the analysis. This report contains the necessary modifications to the analysis of Ref. 15.

The full state simulation, contained in this report consists of forty-nine(49) degrees of freedom, including the actuator and the control surface. In order to obtain a more practical representation for use in control system lab work, a reduced state model is developed using the method of residualization.

Finally a frequency response technique is developed, using the output of an accelerometer and a measurement of control surface rotation, driven by an oscillating electric current input at the hydraulic actuator control valve, as a device for checking the actuator-wing simulation model and to calibrate the flutter suppression feed-back law.

An additional analytic effort directed toward reducing the number of degrees of freedom and the development of a control law for real time flutter suppression is contained in Ref. 16.

## I. Description of the Wing Flutter Model

The DAST ARW-1 wing was designed at the Langley Research Center as a swept back, cantilevered wind tunnel flutter model of a prototype, remotely-piloted, drone aircraft used to study active control concepts including flutter suppression. The data used in this report for determining the inertial and structural characteristics of the wing, as well as the results of vibration and wind tunnel flutter tests, were furnished by Mr. R. Doggett of NASA/LaRC.

The geometric planform and dimensions of the wing are shown in Fig. 1. The leading edge has a sweep back angle of  $44.32^\circ$ . The wing has a taper ratio of .392 and an aspect ratio of 6.4. The airfoil is a NACA 65A10 section. The main structural beam is a single tapered aluminum bar construction with a cruciform cross section (see Fig. 2). The dimensions of the spar cross section at various locations along the length are shown in Table 1. The measured stiffness distribution is shown in Fig. 3 in terms of the bending and torsional stiffness, EI and GJ curves.

The wing is divided into eight pod sections by means of seven ribs oriented in the stream direction (see Fig. 4). Each section contains concentrated masses rigidly connected to the main beam to provide realistic mass offsets with respect to the local elastic axis. A more thorough description of the wing model is contained in Ref. 15.

A control surface is provided along the trailing edge, equipped with an electro-hydraulic servo-actuator. The surface hinge line is located at 80% of the local streamwise chord. The reaction torques of the actuator are constrained by a link to the main structural beam in the control surface pod section. This report contains the modifications to the analysis required to simulate the hydraulic and structural constraints.

A Cartesian coordinate system is used in the analysis. The origin of the system is at the intersection of the wing root chord and the wing leading edge. The x-axis is positive forward in the streamwise direction. The z-axis is positive down, and the y-axis forms a right hand system. (See Fig. 4). The structural axis of the beam defines the y' coordinate, rotated at an angle of  $40.7^\circ$  with respect to the y-axis. The origin of the x', y', z' system is at (-.372364, 0., 0.).

Thus

$$\begin{Bmatrix} x' \\ y' \\ z' \end{Bmatrix} = \begin{pmatrix} \cos\theta & \sin\theta & 0 \\ -\sin\theta & \cos\theta & 0 \\ 0 & 0 & 1 \end{pmatrix} \begin{Bmatrix} x + .372364 \\ y \\ z \end{Bmatrix} \quad (1)$$

where  $\theta = 40.7^\circ$ .

The dynamical coordinates are located along the  $y'$  axis (see Fig. 5). These consist of seven vertical deflections,  $h(y'_i)$  ( $i = 1, 7$ ), seven rotations in the air stream direction,  $\alpha(y'_i)$  ( $i = 1, 7$ ), a rotation,  $\sigma_H$ , about the control surface hinge line representing the actuator housing constrained by structural link to the wing beam, and a rotation,  $\delta$ , about the hinge line representing the control surface deflection. The dynamical coordinates form a  $16 \times 1$  vector,  $w$ , defined by

$$\begin{Bmatrix} w \end{Bmatrix}_{16 \times 1} = \begin{Bmatrix} h_1 \\ h_2 \\ \cdot \\ \cdot \\ h_7 \\ \alpha_1 \\ \cdot \\ \cdot \\ \alpha_7 \\ \sigma_H \\ \delta \end{Bmatrix}_{16 \times 1} \quad (2)$$

The equations of motion will be generated in terms of the forces and moments affecting these 16 degrees-of-freedom. The center line, or root section, is constrained to maintain zero deflection in the vertical direction and in streamwise rotation. Thus  $h(0) = \alpha(0) = 0$ .

## II. Structural Influence Coefficients

The structural influence coefficients were computed utilizing the SPAR computer program at the LaRC computer facility. The SPAR program requires that the wing be decomposed into a series of grid points. At each point, six degrees-of-freedom are permitted. There are three translations along, and three rotations about each of the three axes. A finite element method is employed to compute the linear relationships between the deformations of the grid points with respect to one another and the resulting forces and moments resisting these deformations. For the DAST wing, a grid decomposition of 111 points was used, resulting in 666 degrees-of-freedom. (See Figure 6). Of these, points 103 through 109 correspond to the concentrated masses which undergo rigid motions without relative structural deformations. Point 111 is the control surface linkage constraint for rotation about the hinge line.

To produce the structural influence coefficients for the 16 degrees-of-freedom defined by the dynamical coordinate vector,  $w$ , we constrained 7 points in 2 degrees-of-freedom (vertical deflection and rotation in the flight direction). The 15th degree-of-freedom is constrained to be a pure rotation about the control surface hinge line. The 16th degree-of-freedom, defining the control surface rotation, is constrained by the compression of the actuator hydraulic fluid and is computed independently of the beam influence coefficients.

All other degrees-of-freedom in the original SPAR deformation are left unconstrained except for the root section grid points (97, 100 and 102) which are constrained in three directions. (See Figure 7). The SPAR program solves a static equilibrium problem for which one coordinate of  $w$  is set equal to unity, and the other twenty-three are constrained to be zero. The forces and moments at the 24 locations are computed by solving a set of 24 equations of equilibrium. Thus, we have

$$\begin{Bmatrix} F_\ell \\ M_\ell \\ F_{0,\ell} \\ M_{0,\ell} \end{Bmatrix}_{24x1} = \begin{Bmatrix} K_{15x15} & k_{i,16} \cdot k_{i,24} \\ k_{16,j} \\ k_{24,j} \end{Bmatrix}_{24x24} \begin{Bmatrix} 0 \\ \vdots \\ 0 \\ 1 \\ 0 \\ \vdots \\ 0 \end{Bmatrix}_{24x1} \quad (3)$$

where the  $\ell$ th element of  $w$ ,  $w_\ell$ , = 1 and all other elements, including  $h(0)$  and  $\alpha(0)$ , are set equal to zero. The forces,  $F_{0,\ell}$ , and the moments,  $M_{0,\ell}$ , are the reactions at the root section required to hold the root section undeformed.

The elements of the  $\ell$ th column of the influence coefficient matrix ( $K$ ) are given by

$$\left\{ k_{i,\ell} \right\}_{15 \times 1} = \left\{ \begin{matrix} F_\ell \\ M_\ell \end{matrix} \right\}_{15 \times 1} \quad (3a)$$

The deflections at the remaining 642 grid points are left unconstrained. The beam matrix of influence coefficients is given in the first 15 rows and columns of Table 2. The units are in Newtons per meter of deflection, Newtons per radian, Newton-meters per meter of deflection and Newton-meters per radian arranged as follows:

$$\left( \begin{array}{c|c} \text{Newtons/meter (7x7)} & \text{Newtons/rad (7x8)} \\ \hline \text{Newton-meter/meter (8x7)} & \text{Newton-meter/rad (8x8)} \end{array} \right) \quad (4)$$

To obtain the elements of the 16th row and column, we note that the relative rotation of actuator vane with respect to the actuator housing is resisted by compression of the hydraulic fluid. The fluid bulk modulus,  $\beta$ , is related to the change in pressure and the percentage change in volume by the equation

$$\beta = -\frac{\Delta p}{\Delta V_0/V_0} \quad (5a)$$

The resisting torque is related to the pressure difference across the actuator vane, by the equation

$$T = (p_1 - p_2) \frac{\ell(r_1^2 - r_2^2)}{2} \quad (5b)$$

where

- $\ell$  = length of actuator vane
- $r_1$  = outer radius of the actuator vane
- $r_2$  = inner radius of the actuator vane
- $V_o$  = volume of the fluid
- $\Delta V_o$  = change in fluid volume due to compression

Since the pressure difference is twice the compression pressure change,  $\Delta p$ , we have for the actuator torque,  $T$ , the expression,

$$T = 2 \Delta p C_A \quad (5c)$$

where

$$C_A = \frac{\ell (r_1^2 - r_2^2)}{2} \quad (5d)$$

The change in volume, in the actuator chamber,  $\Delta V_o$ , is related to the relative rotation of the vane with respect to the housing by the equation

$$\Delta V_o = \Delta (\delta - \theta_H) C_A \quad (5e)$$

Thus, we have

$$\frac{T}{\Delta(\delta - \theta_H)} = \frac{2 C_A^2 \beta}{V_o} \quad (5f)$$

and

$$k_{15,16} = k_{16,15} = -k_{16,16} = -\frac{2 C_A^2 \beta}{V_o} \quad (5g)$$

The remaining terms of  $k_{16,i} = k_{i,16} = 0$ . for  $i = 1$  through 14.

For the proposed actuator we have

$$k_{16,16} = 19.887816 \text{ Newton meters/rad}$$

Table 2 contains the actuator housing/structural beam constraint.

$$k_{15,15} = .81689104(10)^4 \text{ Newton meters/rad} \quad (5h)$$

### III. Mass Data

The SPAR program carries out a vibration analysis of the DAST wing by solving an eigenvalue problem utilizing the input mass and stiffness data at the 111 grid points. Of the 666 degrees-of-freedom, 18 at the root section (grid points 97,100 and 102) are constrained to be fixed, and 42 correspond to the 7 rigidly attached concentrated masses (103 through 109). For the purposes of this study, the number of degrees-of-freedom has been reduced to 16. In order to produce a simulation in which the significant vibration modes are well represented, it is necessary to compute a set of lumped masses at the c.g.'s of the seven sections, which, together with the rigid concentrated masses and the  $16 \times 16$  influence coefficient matrix, will reproduce the significant low-order vibration modes.

To accomplish this, the distributed beam and plate masses have been summed in 7 sections and are listed in Table 3. The concentrated masses are listed in Table 4.

The combined masses and mass moments of inertia (in the mks system) of Table 3 and 4 form the first 14 diagonal elements of the mass matrix shown in Table 5. The mass moment of inertia of the actuator housing is given in Table 5 as the 15th diagonal element. To obtain the mass moment of inertia of the 16 degree-of-freedom we must add to the moment of inertia of the control surface,  $m_{\delta}$ , the equivalent inertia of the trapped hydraulic fluid,  $I_{EQ}$ . The sum is listed in Table 5 as the  $m_{16,16}$  element.

#### IV. Frequencies and Modes

To ensure that the SPAR representation of the DAST cantilevered wing is a valid simulation of the wind tunnel model, a comparison of the first four computed and measured vibration modes was carried out using the full 111 grid-point model. Figure 8 contains the results of the vibration test furnished by R. Doggett of NASA/LaRC. Figures (9a), (9b), (9c), and (9d) are plots of the same modes with the SPAR program using all of the 111 grid points. The comparison is seen to be good. Figures 10 and 11 contain the next two highest modes obtained by the SPAR program for which no vibration data is available.

Finally, in order to test the validity of the reduced 16 degrees-of-freedom model, an eigenvalue analysis using the mass, M, and influence coefficient, K, matrices was carried out. For the purposes of the vibration analysis comparison, the actuator hydraulic pressure is assumed to be acting, however the feed back is left in the open loop mode. The results of the analysis are shown in Figures (12a), (12b), (12c), and (12d), for the first four modes. The agreement is seen to be good. The 16 degrees-of-freedom eigenvalues are shown in Table 6 together with the vibration test frequencies and those frequencies obtained with the full 666 degrees-of-freedom.

## V. The SOUSSA Program and the Pade' Approximants

The SOUSSA digital program (Refs. 8,9) computes generalized aerodynamic forces for a wing of given planform executing sinusoidal oscillations in a fixed wing deflection mode shape. The generalized forces are computed at a given Mach number,  $m$ , for a given non-dimension frequency,  $k = \frac{\omega b}{v}$ , a characteristic length,  $b$ , and a non-dimensional time variable  $T = \frac{v}{b} t$ . The generalized forces are given in terms of the force per unit dynamic pressure,  $q$ . Thus we have

$$\left\{ \frac{\bar{L}(j\omega)}{q} \right\} = (Q_R(m,k) + j Q_I(m,k)) \left\{ \bar{W}(j\omega) \right\} \quad (6)$$

where  $j = \sqrt{-1}$  and  $\bar{W}(j\omega)$  is the non-dimensional deflection mode shape oscillating at the sinusoidal frequency,  $\omega$ .

In the application we seek in this study, we desire to obtain the aerodynamic forces in influence coefficient form. To obtain this, a pre-processor was developed by Prof. L. Morino to generate 15 unit impulse function modes, one for each of the first 14 degrees-of-freedom of our  $w$  vector, plus one for the control surface rotation about the hinge line. The actuator housing rotation,  $\sigma_H$ , is assumed to produce no aerodynamic forces. For the purposes of convenience we retain the  $\bar{W}$  vector as a 16x1, and the corresponding generalized force vector,  $\bar{L}/q$ , as a 16x1 with the proviso that the 15 element of the generalized force vector is known to be identically zero. Thus, for the  $i$ th unit impulse function mode we have unit deflection for the  $i$ th element and zeroes for the other 15 elements.

We obtain the  $i$ th column of the desired aerodynamic influence coefficient matrix from Eq. (6)

$$\left\{ \frac{\bar{L}(j\omega)}{q} \right\}_i = \left\{ q_{Ri}(m,k) + j q_{Ii}(m,k) \right\} \quad (7)$$

The SOUSSA coordinate system is positive deflection upward, and a positive angle of attack is trailing edge upward. Consequently, we have

$$\left\{ \bar{W}(j\omega) \right\}_{16 \times 1} = - \begin{Bmatrix} h_1(j\omega)/b \\ \vdots \\ h_7(j\omega)/b \\ \alpha_1(j\omega) \\ \vdots \\ \alpha_7(j\omega) \\ \sigma_H(j\omega) \\ \delta(j\omega) \end{Bmatrix}_{16 \times 1} \quad (7a)$$

By choosing the characteristic length  $b$  to be unity, we have

$$\left\{ \bar{W}(j\omega) \right\} = - \left\{ \bar{W}(j\omega) \right\} \quad (7b)$$

Following the method of Pade' approximants, we define a  $16 \times 1$  unsteady aerodynamic force vector (per unit dynamic pressure),  $\dot{x}_p$ , in the real time domain, to satisfy the following matrix differential equation

$$\left\{ \dot{\dot{x}}_p \right\} - (F_p) \left\{ \dot{x}_p \right\} = (H_1) \left\{ \bar{W} \right\} + (H_2) \left\{ \dot{\bar{W}}_2 \right\} + (H_3) \left\{ \ddot{\bar{W}}_3 \right\} \quad (8)$$

where the matrices  $F_p$ ,  $H_1$ ,  $H_2$ , and  $H_3$  are of dimension  $16 \times 16$  and are to be determined.

The SOUSSA generalized force is positive upward, and the generalized moment is positive for a positive (upward) force acting aft of the rotation axis. Thus, we have

$$\left\{ \bar{x}_p(j\omega) \right\} = - \left\{ \frac{\bar{L}(j\omega)}{q} \right\} \quad (9)$$

Finally, we have from the relation between time,  $t$ , and  $T$

$$\frac{d}{dt} \left\{ \bar{W}(j\omega) \right\} = - \frac{v}{b} \frac{d}{dT} \left\{ \bar{W}(j\omega) \right\} \quad (10)$$

and

$$\frac{d^2}{dt^2} \left\{ \bar{W}(j\omega) \right\} = - \left( \frac{v}{b} \right)^2 \frac{d^2}{dT^2} \left\{ \bar{W}(j\omega) \right\}$$

The resulting unsteady lift,  $\bar{x}_p(j\omega)$ , for the non-dimensional sinusoidal  $\bar{W}(j\omega)$  vector is given by the Laplace transform of Eq. (8).

$$\left\langle \bar{x}_p(j\omega) \right\rangle = - \left( j \frac{v}{b} k I - F_p \right)^{-1} \left( H_1 + j \frac{v}{b} k H_2 - \left( \frac{v}{b} k \right)^2 H_3 \right) \left\langle \bar{W}(j\omega) \right\rangle \quad (11)$$

and from Eq.'s (6) and (9) we have

$$\left\langle \bar{x}_p(j\omega) \right\rangle = - \left( Q_R(m, k) \right) + j Q_I(m, k) \left\langle \bar{W}(j\omega) \right\rangle \quad (12)$$

It then follows that

$$\left( j \frac{v}{b} k I - F_p \right)^{-1} \left( H_1 + j \frac{v}{b} k H_2 - \left( \frac{v}{b} k \right)^2 H_3 \right) = Q_R(m, k) + j Q_I(m, k) \quad (13)$$

To determine the desired constant matrices, independent of time and frequency, we have recourse to the Pade' Approximants of Ref.'s 7,11,12,13. In what follows below, we lean heavily on the work of Edwards in Ref. 12.

Since there are four(4) unknown matrices to be determined, we can, at most, satisfy only four(4) conditions. For the first condition, we choose to satisfy Eq. (13) at  $k = 0$ . We have

$$H_1 = - F_p Q_R(m, 0) \quad (14)$$

For the second condition, we choose to determine  $H_3$  from the real part of Eq. (13) giving

$$H_3 = \left( \frac{b}{vk} \right)^2 F_p \left( Q_R(m, k) - Q_R(m, 0) \right) + \left( \frac{b}{vk} \right) Q_I(m, k) \quad (15)$$

As  $k$  increases beyond bound, we have the piston theory limit (Ref. 17)

$$H_3 = \frac{b}{v} Q_{\text{piston}}(m) \quad (b = 1.) \quad (16)$$

The nonzero elements of  $Q_{\text{piston}}$ ,  $q_{ij}$ , are given by ( $i = 1, 7$ )

$$q_{i,i} = -\frac{4\alpha}{m} \left( \frac{c_i^2 - c_{i+1}^2}{2} \right)$$

$$q_{i,i+7} = -\frac{4\alpha}{m} \left( \frac{c_i^3 - c_{i+1}^3}{3} \right) \left( \frac{1 - 2x_o}{2} \right)$$

$$q_{i+7,i} = q_{i,i+7}$$

$$q_{i+7,i+7} = -\frac{4\alpha}{m} \left( \frac{c_i^4 - c_{i+1}^4}{4} \right) (i - 3x_o + 3x_o^2) \quad (16a)$$

$$q_{6,16} = -\frac{4\alpha}{m} \left( \frac{c_6^3 - c_7^3}{3} \right) (1 - x_1) (1 + x_1 - 2x_o)$$

$$q_{13,16} = -\frac{4\alpha}{m} \left( \frac{c_6^4 - c_7^4}{4} \right) \left( 1 - \frac{x_1^3}{3} - \frac{1 - x_1^2}{2} (x_o + x_1) + x_o x_1 (1 - x_1) \right)$$

$$q_{16,6} = q_{6,15}$$

$$q_{16,13} = q_{13,15}$$

$$q_{16,16} = -\frac{4\alpha}{m} \frac{c_6^4 - c_7^4}{4} \frac{1-x_1^3}{3}$$

where

$$\alpha = \frac{1.9431}{.8764016 - .3431794}$$

$c_i$  = wing chord in stream direction at the start of the  $i$ th section

$x_o$  = elastic axis in % chord  $(.4231)$

$x_1$  = hinge line axis in % of chord  $(.80)$

The values of the  $C_i$  are

i	$C_i$ (meters)
1	.8353
2	.7534
3	.6784
4	.6087
5	.5390
6	.4697
7	.4205
8	.3432

We choose as our third condition to match the imaginary part of Eq. (13) to the SOUSSA output for the flutter-reduced frequency,  $k_f$ . Thus we have

$$H_2 = Q_R(m, k_f) - \frac{F_p Q_I(m, k_f)}{k_f} \left( \frac{V}{b} \right) \quad (17)$$

Finally, following the method of Jones, (Ref. 18), we choose for  $F_p$  a diagonal matrix to provide stable poles for the homogeneous differential differential equation for the  $x_p$  vector. We choose for  $F_p$  a diagonal matrix whose elements are given by

$$\begin{aligned} F_{pi,i} &= -\sigma v / b_i \\ F_{p,i+7,i+7} &= F_{p,i,i} \quad i = 1, 7 \\ F_{p,15,15} &= \text{arbitrary large value } (1(10)^7) \\ F_{p,16,16} &= -\sigma v / b_\delta \end{aligned} \quad (18)$$

where

$$\begin{aligned} b_i &= \text{semi chord of the } i\text{th section} \\ b_\delta &= \text{semi chord of control surface} \\ \sigma &= .67034 \end{aligned}$$

The values of the semi chords for the DAST wing, in meters, are given below:

$$\begin{aligned} b_1 &= .39708 \\ b_2 &= .35630 \\ b_3 &= .32215 \end{aligned}$$

$b_4 = .28660$   
 $b_5 = .25244$   
 $b_6 = .21759$   
 $b_7 = .18622$   
 $b_8 = .05049$

The matrices  $H_1$ ,  $H_2$ ,  $H_3$  and  $F_p$  are contained in Tables 7,8,9, and 10 respectively. It should be noted that the rotation of the actuator housing,  $\theta_H$ , ( $w_{15}$ ) produces no aerodynamic forces.

## VI. The Hydraulic Actuator and the Hydro-Electro Valve System

Figure 13 illustrates the manner in which hydraulic fluid pressure applies a torque producing relative change in rotation between the vane/control surface and the housing.

The Equation of motion for the housing is given by

$$m_{15} \frac{d^2}{dt^2} w_{15} + r_{15} \frac{d}{dt} w_{15} = - \sum_{i=1}^{15} k_{15,i} w_i - T \quad (19)$$

where

$r_{15}$  is the structural damping produced by the relative rate of motion between the housing and the wing beam

$k_{15,i}$  are the elements of the 15th row of the structural influence coefficient matrix

$T$  is the torque reaction supplied by hydraulic fluid compression

The equation of motion of the control surface is given by

$$(m_{16} + I_{EQ}) \ddot{w}_{16} + r_{16} \dot{w}_{16} = T + \text{Aerodynamic terms} \quad (20)$$

where

$r_{16}$  the damping supplied by fluid leakage, valve stabilization, etc. designed to produce .30 critical damping (See Ref. 14)

$I_{EQ}$  the effective rotary inertia of the hydraulic fluid

The hydraulic fluid, passing through the electro-servo valve per unit of time, is defined as  $Q_A$ . Since the quantity of fluid must be conserved, it is convenient to divide the flow rate into two factors. The first, is the flow which accommodates the volumetric time rate of change due to the control surface rotation. This portion is modeled as an incompressible fluid flow rate and is proportional to the time rate of change of the relative rotation between the actuator vane and the actuator housing. The second is modeled as that portion of the fluid flow volume which is contained in the time rate of change of the compression in the actuator chamber. This compression produces fluid

pressure, which in turn produces a reaction torque,  $T$ , which accelerates the actuator vane and the attached control surface. We have

$$Q_A = C_A/k_{16,16} \frac{d}{dt}(T + k_{16,16}(w_{16} - w_{15})) \quad (21)$$

We now define the quantity,  $T_{DEF}$ , to be the torque deficiency, given by

$$T_{DEF} = T + k_{16,16}(w_{16} - w_{15}) \quad (22)$$

Eq's. (19) and (20) now may be written as

$$m_{15} \frac{d^2}{dt^2} w_{15} + r_{15} \frac{d}{dt} w_{15} = - \sum_{i=1}^{15} k_{15,i} w_i + k_{16,16}(w_{16} - w_{15}) - T_{DEF} \quad (19a)$$

$$(m_{16} + I_{EQ}) \frac{d^2}{dt^2} w_{16} + r_{16} \frac{d}{dt} w_{16} = T_{DEF} - k_{16,16}(w_{16} - w_{15}) + \text{Aero} \quad (20a)$$

Eq's. (19a) and (20a) contain the derivation of the desired stiffness terms for the structural influence coefficient matrix given in Eq's. (5g) and (5h).

To complete the feed back loop, we now model the electro servo valve as a first order command system.

$$\frac{d}{dt} T_{DEF} = \gamma (T_{DEF} - T_{COM}) \quad (23)$$

where  $\gamma = -\frac{1}{214}$ . (Ref. 1)

and  $T_{COM}$  is the command feed back control torque.

## VII. Equations of Motion

The forces acting on the wing in the air speed region containing the flutter speed are assumed to consist of the following:

- (a) inertia
- (b) unsteady aerodynamic forces
- (c) structural restraint to wing deformation
- (d) random aerodynamic forces due to wind gusts
- (e) a stabilizing feed back torque acting on the control response
- (f) aerodynamic forces due to the control surface deflection

To simulate these forces, assuming small deflections, we require the dynamic coordinate vector,  $w$ , its first and second time derivatives,  $\dot{w}$  and  $\ddot{w}$ , the unsteady aerodynamic force vector  $x_p$ , its time derivative,  $\dot{x}_p$ , the three scalar random gust variables,  $x_{1D}$ ,  $x_{2D}$  and  $\tilde{w}_g$ , the actuator deficiency torque,  $T_{DEF}$ , and feed back control torque,  $T_{COM}$ .

To simulate the system we define a 51 degree of freedom state vector,  $z$ .

Let  $z$  be defined by

$$\left\{ z \right\}_{51 \times 1} = \begin{Bmatrix} w_{16 \times 1} \\ \dot{w}_{16 \times 1} \\ x_p_{16 \times 1} \\ T_{DEF} \\ x_{1D} \\ x_{2D} \end{Bmatrix}_{51 \times 1} \quad (24)$$

The equation of motion for this plant is given by

$$(A_1)_{51 \times 51} \frac{d}{dt} \{z\}_{51 \times 1} = (A_2)_{51 \times 51} \{z\}_{51 \times 1} + \{B\}_{51 \times 1} T_{COM} + \{C\}_{51 \times 1} \tilde{w}_g \quad (25)$$

where

$$(A_1) = \begin{pmatrix} I & 0 & 0 & 0 & 0 & 0 \\ 0 & M & 0 & 0 & 0 & 0 \\ 0 & -H_3 & I & 0 & 0 & 0 \\ 0 & 0 & 0 & 1 & 0 & 0 \\ 0 & 0 & 0 & 0 & 1 & 0 \\ 0 & 0 & 0 & 0 & 0 & 1 \end{pmatrix}_{51 \times 51} \quad (25a)$$

The matrices  $I$ ,  $M$ ,  $H_3$  are all  $16 \times 16$

$$(A_2) = \begin{pmatrix} 0 & I & 0 & 0 & 0 & 0 \\ -K & -D_w & qI & E & F & H \\ H_1 & H_2 & F_p & 0 & 0 & 0 \\ 0 & 0 & 0 & \gamma & 0 & 0 \\ 0 & 0 & 0 & 0 & 0 & 1 \\ 0 & 0 & 0 & 0 & g_2 & h_2 \end{pmatrix}_{51 \times 51} \quad (25b)$$

The matrices  $K$ ,  $D_w$ ,  $H_1$ ,  $H_2$ ,  $F_p$  are  $16 \times 16$   
 $E$ ,  $F$ , and  $H$  are  $16 \times 1$  vectors

All the elements of  $E$  are zero except for  $E_{15} = -1.$ , and  $E_{16} = 1.$

$$\{F\}_{16 \times 1} = (Q_R(m, 0)) \begin{Bmatrix} 1 \\ 1 \\ 1 \\ 1 \end{Bmatrix}_{16 \times 1} .13 \frac{Vq}{C^2}$$

(The matrix,  $Q_R(m, 0)$  is listed in Table 11)

$$g_2 = - \frac{V^2}{C^2} .13$$

$$\{H\}_{16 \times 1} = (Q_R(m, 0)) \begin{Bmatrix} 1 \\ 1 \\ 1 \\ 1 \end{Bmatrix}_{16 \times 1} .565 \frac{q}{C}$$

$$h_2 = - \frac{V}{C} 1.13$$

$$C = 1/2 \text{ the wing MAC } (C = .2524379 \text{ meters})$$

All the elements of the vector  $\{B\}$  are zero except that  $B_{49} = -\gamma$ .

Finally all the elements of the vector  $\{C\}$  are zero except that  $C_{51} = 1$ . The scalar,  $\tilde{w}_g$ , is a variable representing the random gust magnitude. (See Ref. 14 for details).

To obtain a good model for the structural damping matrix,  $D_w$ , we make use of the approximation that the structure provides approximately .5% of critical damping.

Thus, for the case of zero dynamic pressure ( $q = 0$ ), let

$$M^{-1} K = U (\omega_i^2) U^{-1} \quad (25d)$$

where the matrix  $U$  is the matrix of eigenvectors of  $M^{-1} K$  and  $\omega_i^2$  is the diagonal matrix of the eigenvalues. We have as a good approximation of  $D_w$ ,

$$D_w = .01 (M) U (\omega_i) U^{-1} \quad (25e)$$

where  $\omega_i$  is a diagonal matrix of the square roots of the eigenvalues of Eq. (25d). The matrix  $D_w$  is given in Table 12.

To facilitate the analysis, we first invert the  $(A_1)$  matrix and write Eq. (25) in the form

$$\frac{d}{dt} \left\{ z \right\} = \begin{pmatrix} 0 & I & 0 & 0 & 0 & 0 \\ -M^{-1}K & -M^{-1}D_w & qM^{-1} & M^{-1}E & M^{-1}F & M^{-1}H \\ H_1 - H_3 M^{-1}K & H_2 - H_3 M^{-1}D_w & F_p + qH_3 M^{-1} & H_3 M^{-1}E & H_3 M^{-1}F & H_3 M^{-1}H \\ 0 & 0 & 0 & \gamma & 0 & 0 \\ 0 & 0 & 0 & 0 & 0 & 1 \\ 0 & 0 & 0 & 0 & g_2 & h_2 \end{pmatrix} \left\{ z \right\} \quad 51 \times 51$$

$$+ A_1^{-1} \{B\}_{51 \times 1} {}^T_{COM} + A_1^{-1} \{C\}_{51 \times 1} \tilde{w}_g \quad (26)$$

where

$$A_1^{-1} = \begin{pmatrix} I & 0 & 0 & 0 & 0 & 0 \\ 0 & M^{-1} & 0 & 0 & 0 & 0 \\ 0 & H_3 M^{-1} & I & 0 & 0 & 0 \\ 0 & 0 & 0 & 1 & 0 & 0 \\ 0 & 0 & 0 & 0 & 1 & 0 \\ 0 & 0 & 0 & 0 & 0 & 1 \end{pmatrix}_{51 \times 51} \quad (26a)$$

Eq. (26) represents the simulation of the full state. For open loop analysis we may set the feed back control variable,  $T_{COM}$ , to zero. To check the accuracy of the model we obtain the eigenvalues of the homogeneous system (with  $\tilde{w}_g$  and  $T_{COM}$  set to zero) as a function of the dynamic pressure,  $q$ ; and compare the value of  $q$  at flutter with the flutter results obtained by wind tunnel tests.

### VIII. Open Loop Flutter Analysis

The results of the open loop flutter analysis of the DAST wing using the influence coefficient method was carried out by determining the eigenvalues of the homogeneous part of the differential matrix equation (26) for different values of the dynamic pressure,  $q$ , for a fixed Mach number ( $m = .897$ ) and fixed airspeed ( $v = 136 \text{ m/sec}$ ).

The results of the study, shown in Figure 14, are to be compared to a similar plot taken from Ref. 1 shown in Figure 15. In order to illustrate a more detailed comparison of the pertinent flutter modes, we have Fig. 16 which is a plot of the frequency and damping versus dynamic pressure for the open loop system.

The wind tunnel results as obtained from R. Doggett were

$$\begin{aligned}m &= .897 \\q &= 5.36 \text{ kPa} \\v &= 136 \text{ m/sec} \\w &= 8.0 \text{ Hz}\end{aligned}$$

The comparison is shown to be good with both the wind tunnel data and the analytical prediction of Abel (Ref. 1).

## IX. Flutter Suppression Utilizing the Complete Model

The transformation of the physical state vector,  $\{z\}$ , to modal coordinates,  $\{u\}$ , is realized through a  $51 \times 51$  complex matrix,  $T$ .

Let,

$$\{z\} = (T) \{u\} \quad (27)$$

This transformation rotates the matrix  $(A_1^{-1} A_2)$  into canonical form. Thus,

$$T^{-1} (A_1^{-1} A_2) T = (\lambda) \quad (28)$$

where the diagonal elements of  $(\lambda)$  are the real or complex eigenvalues of the matrix  $(A_1^{-1} A_2)$ .

Following the method outlined in Ref. 14 we obtain a more convenient form of the transformation,  $T$ , in real form, we use the transformation,  $Y$ . We generate  $Y$  from  $T$  as follows:

If an eigenvalue is complex, then there exists a related conjugate eigenvalue. Thus if

$$\lambda_i = \alpha_i + j \omega_i \quad (28a)$$

$$\text{then } \lambda_{i+1} = \alpha_i - j \omega_i \quad (28b)$$

$$\text{where } j = \sqrt{-1} \quad (28c)$$

If the corresponding eigen vector of  $\lambda_i$  and  $\lambda_{i+1}$  are  $\{t_i\}$ , and  $\{t_{i+1}\}$  where

$$\{t_i\} = \{p_i\} + j \{q_i\} \quad (28d)$$

and

$$\{t_{i+1}\} = \{p_i\} - j \{q_i\} \quad (28e)$$

A real equivalent of Eq. (27) is given by

$$\{z\} = (Y) \{u\} \quad (28f)$$

where

$$\{y_i\} = \{p_i\} \quad (28g)$$

and

$$\{y_{i+1}\} = \{q_i\} \quad (28h)$$

In the event that the  $i$ th characteristic root of  $(A_1^{-1}A_2)$  is real, then we choose the eigen vector so that

$$\{y_i\} = \{p_i\} \quad (28i)$$

The corresponding elements in the canonical real Jordon matrix  $(\omega)$  are given by

If the roots are  $\alpha_i \pm \omega_i$ , then

$$\begin{aligned}\omega_{i,i} &= \alpha_i \\ \omega_{i,i+1} &= \omega_i \\ \omega_{i+1,i} &= -\omega_i \\ \omega_{i+1,i+1} &= \alpha_i\end{aligned} \quad (28j)$$

and if the  $i$ th root is real then we have

$$\omega_{i,i} = \alpha_i \quad (28k)$$

The eigen vector transformation  $(Y)_{51 \times 51}$  is listed in Table 13 for the base case of Mach number = .897 and a dynamic pressure of  $q = 8.0 \text{ kPa}$ . The corresponding eigen values are given in Table 14.

The modal form for the full 51 DOF system is given by

$$\begin{aligned}\frac{d}{dt} \{u\} &= (\omega) \{u\} + (Y)^{-1} (A_1)^{-1} \{B_i\}_{COM}^T \\ &\quad + (Y)^{-1} (A_1)^{-1} \{C\} \tilde{w}_g\end{aligned} \quad (29)$$

Examination of Table 14 indicate that the first two complex eigen values have real positive parts and are unstable. Fig. (14) indicates that the open loop flutter  $q$  occurs somewhat earlier than  $q = 8.0 \text{ kPa}$  at a dynamic pressure of  $q_{FLUTTER} = 5.36 \text{ kPa}$ . To suppress the flutter condition we design a feed back gain for  $T_{COM}$  to place the unstable pole at a desired location in the stable, negative real half plane. The method for accomplishing this is developed in Ref. 14 and described herein.

Let the unstable pair of coupled equations ( $u_1$  and  $u_2$ ) of Eq. (29) be given by

$$\frac{d}{dt} \begin{Bmatrix} u_1(t) \\ u_2(t) \end{Bmatrix} = \begin{pmatrix} \alpha_1 \omega_1 \\ \omega_1 \alpha_1 \end{pmatrix} \begin{Bmatrix} u_1(t) \\ u_2(t) \end{Bmatrix} + \begin{Bmatrix} \ell_1 \\ \ell_2 \end{Bmatrix} T_{COM} \quad (30)$$

where  $\alpha_1$  is positive. In the above we may neglect the random gust  $\tilde{w}_g$  since this external force plays no role in the instability. We choose the command torque,  $T_{COM}$ , to have a fixed constant value over a fixed interval,  $\Delta T$ , and equal to a linear combination of  $u_1(t_1)$  and  $u_2(t_1)$ , where  $t_1$  is the start of the interval  $\Delta T$ . Thus, we have

$$\begin{Bmatrix} \ell_1 \\ \ell_2 \end{Bmatrix}_{T_{COM}} = \begin{pmatrix} f_{11} & f_{12} \\ f_{21} & f_{22} \end{pmatrix} \begin{Bmatrix} u_1(t_1) \\ u_2(t_1) \end{Bmatrix} \quad (31)$$

where the constants,  $f_{11}$ ,  $f_{12}$ ,  $f_{21}$ , and  $f_{22}$  are to be determined. It is plain that the feed back gain is given by

$$T_{COM} = \frac{1}{\ell_1} (f_{11} u_1(t_1) + f_{12} u_2(t_1)) \quad (32)$$

or

$$T_{COM} = \frac{1}{\ell_2} (f_{21} u_1(t_1) + f_{22} u_2(t_1))$$

Thus only two of the four  $f_{ij}$  are independent.

Under the assumption of Eq. (31), Eq. (30) may be written as

$$\frac{d}{dt} \begin{Bmatrix} u_1(t) \\ u_2(t) \end{Bmatrix} = \begin{pmatrix} \alpha_1 \omega_1 \\ -\omega_1 \alpha_1 \end{pmatrix} \begin{Bmatrix} u_1(t) \\ u_2(t) \end{Bmatrix} + \begin{pmatrix} f_{11} & f_{12} \\ f_{21} & f_{22} \end{pmatrix} \begin{Bmatrix} u_1(t_1) \\ u_2(t_1) \end{Bmatrix} \quad (33)$$

Since the non homogeneous forcing function is constant we may integrate Eq. (33) and have at the end of the fixed interval

$$\begin{Bmatrix} u_1(t_1 + \Delta T) \\ u_2(t_1 + \Delta T) \end{Bmatrix} = (B + DF) \begin{Bmatrix} u_1(t_1) \\ u_2(t_1) \end{Bmatrix} \quad (34)$$

where

$$b_{11} = e^{\alpha_1 \Delta T} \cos (\omega_1 \Delta T)$$

$$b_{12} = e^{\alpha_1 \Delta T} \sin (\omega_1 \Delta T)$$

$$b_{21} = -b_{12} \quad (34a)$$

$$b_{22} = b_{11}$$

$$d_{11} = (\omega_1 b_{12} - \alpha_1 (1 - b_{11})) / (\alpha_1^2 + \omega_1^2)$$

$$d_{12} = (\alpha_1 b_{12} + \omega_1 (1 - b_{11})) / (\alpha_1^2 + \omega_1^2)$$

$$d_{21} = -d_{12}$$

$$d_{22} = d_{11}$$

We now define a unique, equivalent  $2 \times 2$  system, with poles in the prescribed location ( $\sigma \pm j\delta$  and  $\sigma > 0$ ) such that

$$\frac{d}{dt} \begin{Bmatrix} \bar{u}_1(t) \\ \bar{u}_2(t) \end{Bmatrix} = \begin{pmatrix} e_{11} & e_{12} \\ e_{21} & e_{22} \end{pmatrix} \begin{Bmatrix} \bar{u}_1(t) \\ \bar{u}_2(t) \end{Bmatrix} \quad (35)$$

and choose  $e_{11}$ ,  $e_{12}$ ,  $e_{21}$ , and  $e_{22}$  so that

$$\begin{aligned} e_{11} + e_{12} &= 2\sigma > 0 \\ e_{11} e_{22} - e_{12} e_{21} &= \sigma^2 + \delta^2 \end{aligned} \quad (36a)$$

and demand of the output at  $t = t_1 + \Delta T$ , that if

$$\bar{u}_1(t_1) = u_1(t_1) \text{ and if } \bar{u}_2(t_1) = u_2(t_1)$$

then at  $t = t_1 + \Delta T$  we require

$$\bar{u}_1(t_1 + \Delta T) = u_1(t_1 + \Delta T) \quad (36b)$$

$$\text{and } \bar{u}_2(t_1 + \Delta T) = u_2(t_1 + \Delta T)$$

The output of Eq. 35 is given by

$$\begin{Bmatrix} \bar{u}_1(t_1 + \Delta T) \\ \bar{u}_2(t_1 + \Delta T) \end{Bmatrix} = [x_1 I + x_2 E] \begin{Bmatrix} \bar{u}_1(t_1) \\ \bar{u}_2(t_2) \end{Bmatrix} \quad (37)$$

where

$$\begin{aligned} x_1 &= e^{\sigma \Delta T} (\cos(\delta \Delta T) - \frac{\sigma}{\delta} \sin(\delta \Delta T)) \\ x_2 &= e^{\sigma \Delta T} \frac{\sin(\delta \Delta T)}{\delta} \end{aligned} \quad (37a)$$

The two systems (Eq. (33) and Eq. (37) are equivalent in the sense that they periodically coincide at every  $\Delta T$  interval provided that

$$B + DF = x_1 I + x_2 E \quad (38)$$

The 8 unknown constants in F and E required to satisfy Eq. (38), Eq. (32) and Eq. (36a) are given by

$$\begin{aligned} e_{11} &= \kappa a_2 - 2\sigma (x_1 - b_{11} - b_{12}/ )/b_{11} \\ e_{22} &= 2\sigma - e_{11} \\ e_{12} &= b_{12}/x_2 + (x_1 + x_2 e_{22} - b_{11})/(v x_2) \\ e_{21} &= -b_{12}/x_2 + (x_1 + x_2 e_{11} - b_{11}) v/x_2 \\ f_{11} &= \frac{\ell_1}{\ell_2} (x_1 + x_2 e_{11} - b_{11}) / ( \frac{\ell_1}{\ell_2} b_{11} + b_{12}) \\ f_{21} &= \frac{\ell_2}{\ell_1} f_{11} \\ f_{22} &= (x_1 + x_2 e_{22} - b_{11}) / (b_{11} - b_{12} \frac{\ell_1}{\ell_2}) \\ f_{21} &= \frac{\ell_1}{\ell_2} f_{22} \end{aligned} \quad (39)$$

where

$$\kappa = \sigma^2 + \delta^2 \quad (39a)$$
$$v = (\ell_2 b_{11} - \ell_1 b_{12}) / (\ell_2 b_{12} + \ell_1 b_{11})$$

The utilization of this form of the stabilizing feed back torque will in general produce a stable system with the poles of  $u_1$  and  $u_2$  at the desired location. The remaining poles of the system will not remain invariant and some shifting will occur, although the entire system in general, will remain stable.

The actuator feed back law requires an estimate of the model state  $u_1$  and  $u_2$  at a periodic sequence of times  $t_0, t_0 + \Delta T, t_0 + 2 \Delta T$ , etc. Since the model state is not directly observable, an estimator (or observer) will be required, based on some known filter method (such as Kalman or complementary). Utilizing the output of some measurable quantities, such as an accelerometer placed at some fixed wing station, we may proceed to estimate the desired canonical states,  $u_1(t)$  and  $u_2(t)$  at the periodic intervals.

For the purposes of this study, which are to predict the response of the actuator-wing combination at various values of dynamic pressure to calibrate the digital feed back law, we will assume that we possess perfect knowledge of the 51 degrees of freedom (neglecting the effect of the external random wind gust,  $\tilde{w}_g$ ).

We now proceed to develop an analytical procedure for testing and calibrating the actuator-wing combination and to determine instrumentation for such a purpose.

## X. Testing and Calibration of the Actuator Feed Back Law

Standard procedures for testing and calibrating wind tunnel models are well known. Static deflection tests to obtain checks on the structural influence coefficients, as well as vibration "shake" tests to obtain the normal modes and frequencies in still air are typical of these methods. A somewhat more sophisticated calibration and test check-out procedure is to use the frequency response of some measurable output of the wing (such as an accelerometer, or a surface rotation) driven by a sinusoidal input at a given amplitude and frequency. This method has the advantage of incorporating the entire system including the interaction of the structural, inertial and aerodynamic subsystems, into a single measurable quantity and which has the advantage of being computable and predictable. By recording the accelerometer and control surface rotation amplitude and phase with respect to the known oscillatory input signal at the actuator valve and comparing this with the predicted amplitude and phase, based on our analytical simulation of the wing/actuator combination, we will be testing the accuracy of our simulation and at the same time calibrating the feed back law. To determine the vertical acceleration of the wing at a point (X, Y), let

$$y_i \leq y \leq y_{i+1} \quad (40)$$

then, the acceleration of the wing  $\ddot{h}(x,y)$  is given by

$$\begin{aligned} \ddot{h}(x,y) &= \ddot{h}_i(x_i, y_i) + \frac{\ddot{h}_{i+1}(x_{i+1}, y_{i+1}) - \ddot{h}_i(x_i, y_i)}{y_{i+1} - y_i} (y - y_i) \\ &\quad + \left( \ddot{\alpha}_i(x_i, y_i) + \frac{\ddot{\alpha}_{i+1}(x_{i+1}, y_{i+1}) - \ddot{\alpha}_i(x_i, y_i)}{y_{i+1} - y_i} (y - y_i) \right) (x - y_{E.A.}(y)) \end{aligned} \quad (41)$$

$$\text{where } y_{E.A.}(y) = -.372364 - .860y \quad (41a)$$

Thus, the value of the acceleration at any point along the wing can be determined from a linear combination of at most 4 coordinates of our physical state.

We choose for the simulation of the frequency response of our 51 degree-of-freedom system the modal description of the state (Eq. (29)).

$$\frac{d}{dt} \langle u(t) \rangle = (\Omega) \langle u(t) \rangle + \langle \ell_i \rangle (T_{COM} + a e^{j\omega t}) \quad (42)$$

where, in Eq. (29), we have set

$$\tilde{w}_g = 0 \quad (42a)$$

and

$$(Y)^{-1} (A_1)^{-1} \langle B_i \rangle = \langle \ell_i \rangle \quad (42b)$$

We choose for the feed back law, the gains obtained in Eq. (32).

$$T_{COM} = \frac{1}{\ell_i} (f_{11} u_1(t_1) + f_{12} u_2(t_1)) \quad (32)$$

$$\text{or } T_{COM} = \frac{1}{\ell_i} (f_{21} u_1(t_1) + f_{22} u_2(t_1))$$

The scalar forcing function,  $a e^{j\omega t}$ , is the oscillatory input to the actuator valve with fixed amplitude,  $a$ , and frequency,  $\omega$ . ( $j = \sqrt{-1}$ ).

We seek to obtain a dynamical system, equivalent to that represented by Eq. (42) in which we replace the piecewise constant feed back control,  $T_{COM}$ , as a continuous function of  $u_1(t)$  and  $u_2(t)$  which coincides with the true  $T_{COM}$  at the time intervals  $t_0, t_0 + \Delta T, t_0 + 2 \Delta T$ , etc. To accomplish this we note that we may invert the  $2 \times 2$  transition matrix of Eq. (37) and obtain

$$\begin{pmatrix} u_1(t_1) \\ u_2(t_1) \end{pmatrix} = \begin{pmatrix} x_1(-\Delta T) I + x_2(-\Delta T) \end{pmatrix} \begin{pmatrix} e_{11} & e_{12} \\ e_{21} & e_{22} \end{pmatrix} \begin{pmatrix} u_1(t_1 + \Delta T) \\ u_2(t_1 + \Delta T) \end{pmatrix} \quad (43)$$

It follows that in the equivalent system

$$T_{COM} = \frac{1}{\ell_i} [f_{11} \ f_{12}] \begin{pmatrix} x_1(-\Delta T) I + x_2(-\Delta T) \end{pmatrix} \begin{pmatrix} e_{11} & e_{12} \\ e_{21} & e_{22} \end{pmatrix} \begin{pmatrix} u_1(t) \\ u_2(t) \end{pmatrix} \quad (44)$$

Our equivalent, homogeneous system becomes

$$\frac{d}{dt} \begin{Bmatrix} u_i(t) \end{Bmatrix} = \begin{pmatrix} E & | & 0 \\ - & P & | & - \\ & & | & \bar{\Omega} \end{pmatrix} \begin{Bmatrix} u_i(t) \end{Bmatrix} + \begin{Bmatrix} \ell_i \end{Bmatrix} a e^{j\omega t} \quad (45)$$

where

$$(E) = \begin{pmatrix} e_{11} & e_{12} \\ e_{21} & e_{22} \end{pmatrix}$$

$(P)_{49 \times 2}$  is a  $49 \times 2$  matrix

and  $(\bar{\Omega})_{49 \times 49}$  is the bottom of our original real Jordon form of Eq. (42).

The elements of  $(P)$  are given by

$$p_{i,1} = \frac{\ell_i}{-\ell_1} (f_{11} (x_1(-\Delta T) + x_2(-\Delta T) e_{11}) + f_{12} x_2 (-\Delta T) e_{21}) \quad (45a)$$

$$p_{i,2} = \frac{\ell_i}{-\ell_1} (f_{11} x_2 (-\Delta T) e_{12} + f_{12} (x_1(-\Delta T) + x_2(-\Delta T) e_{22})) \quad (45b)$$

$$(i = 3, 51)$$

We may now obtain the frequency response of the equivalent modal state  $u(t)$ , to the periodic forcing function  $a e^{j\omega t}$ . Since all the roots of the equivalent system (Eq.(45)) are now stable, we may obtain the steady state frequency response to a sinusoidal input,  $a e^{j\omega t}$ , by

$$\left\{ \frac{d}{dt} u_i(t) \right\} = a \left( j\omega I - \begin{pmatrix} E & | & 0 \\ - & P & | & - \\ & & | & \bar{\Omega} \end{pmatrix} \right)^{-1} \begin{Bmatrix} \ell_i \end{Bmatrix} j\omega e^{j\omega t} \quad (46)$$

To obtain an explicit solution for the inverse of the matrix, we have the following:

Let the matrix  $A(N \times N)$  be given by

$$\begin{pmatrix} E & | & 0 \\ - & P & | & - \\ & & | & \Omega \end{pmatrix}_{(N=51)} = A \quad (N \times N) \quad (47a)$$

Let the characteristic polynomial of  $(\lambda I - A)$  be given by

$$\left| I - \lambda - A \right| = \sum_{k=0}^N \lambda^{N-k} a_k \quad (a_0 = 1) \quad (47b)$$

Let the inverse of  $(I\lambda - A)$  be  $(C)$ . Then  $(C)$  is given by

$$(C) = \frac{1}{\sum_{k=0}^N a_k \lambda^{N-k}} \left( \sum_{k=1}^N \lambda^{N-k} \right) B_k \quad (47c)$$

where the matrices  $B_k$  are obtained by recursion

$$B_1 = a_0 I \quad (47d)$$

$$B_k = a_{k-1} I + AB_{k-1}$$

$$(k = 2, N)$$

We have that every element of the inverse is a rational polynomial

$$c_{ij}(\lambda) = \frac{\sum_{k=1}^N \lambda^{N-k} (b_k)_{i,j}}{\sum_{k=0}^N a_k \lambda^{N-k}} \quad (47e)$$

where  $(b_k)_{i,j}$  is the  $i,j$ th element of  $B_k$

It follows that the time derivative of the  $i$ th modal coordinate is given by

$$\frac{d}{dt} u_i(t) = (jw e^{jw t}) \sum_{k=1}^{51} c_{i,k} (jw) \ell_k \quad (48)$$

To obtain accelerations  $\ddot{h}_i$ ,  $\ddot{h}_{i+1}$ ,  $\ddot{\alpha}_i$  and  $\ddot{\alpha}_{i+1}$  we have recourse to the relationship in Eq. (28f)

$$\{\dot{z}(t)\} = (Y) \{\dot{u}(t)\} \quad (49)$$

so that

$$\begin{aligned}\ddot{h}_i(t) &= \sum_{j=1}^{51} y_{i+7,j} \dot{u}_j(t) \\ \ddot{h}_{i+1}(t) &= \sum_{j=1}^{51} y_{i+8,j} \dot{u}_j(t) \\ \ddot{\alpha}_i(t) &= \sum_{j=1}^{51} y_{i+23,j} \dot{u}_j(t) \\ \ddot{\alpha}_{i+1}(t) &= \sum_{j=1}^{51} y_{i+24,j} \dot{u}_j(t)\end{aligned} \quad (50)$$

Using Eq. (41a) we may obtain the amplitude ratio and phase for the predicted acceleration response to the oscillatory input.

Another measurement which can readily be made is the control surface rotation,  $\delta$ , which is given by the sixteenth element of the  $\{z\}$  vector. We have

$$\delta(t) = z_{16}(t) = \sum_{i=1}^{51} y_{16,i} u_i(t) \quad (51)$$

where

$$u_i(t) = \left( \sum_{k=1}^{51} c_{i,k} (jw)^k \right) e^{j\omega t} \quad (51a)$$

Utilizing the measured and predicted frequency response for an accelerometer and the surface rotation for 3 or 4 values of dynamic pressure (below the flutter  $q$ ) will serve to test the adequacy of the simulation and to calibrate the feed back actuator law.

## XI. Flutter Suppression Utilizing a Reduced State

For the purposes of developing a digital discrete flutter suppression feed back law and to test the electrical circuitry in a control system laboratory it is often convenient to have a reduced simulation model of the full 51 degree-of-freedom model. The most favored technique for state reduction is the method of residualization. In this method, the state is divided into two categories, the slow/low frequency states that are most active in the flutter instability, and those states where natural frequency is too large to affect the flutter instability. The sense in which the fast states are to be neglected, or eliminated, is to set the time deviation of the fast states to zero and to use those differential equations, with zero derivatives, as a means for solving for the fast states as functions of the slow states. In this way, the effect of the fast states on the slow states is maintained in the remaining differential equations and the system is reduced.

For the purposes of arranging the states according to frequency, we choose the real canonical form of this system simulation, Eq. (29).

Let the characteristic roots be arranged in the order of increasing absolute value

$$|\alpha_i + j w_i| \leq |\alpha_{i+1} + j w_{k+1}| \quad (52)$$

(i = 1, 51)

We choose to include in the analysis all canonical states whose absolute characteristic amplitude is less than five(5) times the flutter instability characteristic magnitude. We divide the canonical state  $\{u_i\}$  into two states

$$\frac{d}{dt} \{u_A\} = (\Omega_A) \{u_A\} + \{\ell_A\} T_{COM} + \{\bar{C}_A\} \tilde{w}_g \quad (53a)$$

$$\frac{d}{dt} \{u_B\} = (\Omega_B) \{u_B\} + \{\ell_B\} T_{COM} + \{\bar{C}_B\} \tilde{w}_g \quad (53b)$$

We set

$$\frac{d}{dt} \{u_B\} = 0 \quad (54)$$

and from Eq. (53b) we obtain

$$\{u_B\} = (\Omega_B)^{-1} \{\ell_B\}_{T_{COM}} + (\Omega_B)^{-1} \{\bar{C}_B\} \tilde{w}_g \quad (55)$$

The transformation ( $Y$ ), which carries  $\{u_i\}$  into the physical state  $\{z_i\}$  (Eq. (28f)), may be decomposed into

$$\{z_A\} = (Y_{AA})\{u_A\} + (Y_{AB}) \left\{ (\Omega_B)^{-1} \{\ell_B\}_{T_{COM}} + (\Omega_B)^{-1} \{\bar{C}_B\} \tilde{w}_g \right\} \quad (56a)$$

and

$$\{z_B\} = (Y_{BA})\{u_A\} + (Y_{BB}) \left\{ (\Omega_B)^{-1} \{\ell_B\}_{T_{COM}} + (\Omega_B)^{-1} \{\bar{C}_B\} \tilde{w}_g \right\} \quad (56b)$$

Thus, we may represent the entire 51 physical state vector in terms of the reduced cononical state  $\{u_A\}$  (Eq. 53a) and the non-homogeneous forcing functions  $T_{COM}$  and  $\tilde{w}_g$ .

It should be noted that the real Jordan matrix,  $(\Omega)$ , is a function of the dynamic pressure,  $q$ , for a fixed Mach number,  $M$ . In carrying out the reduced state feed back law development, a sequence of  $(\Omega(q))$  matrices and associated real characteristic transformation  $(Y(q))$  must be processed, so that the digital feed back law will be a function of  $q$  for fixed Mach number,  $M$ .

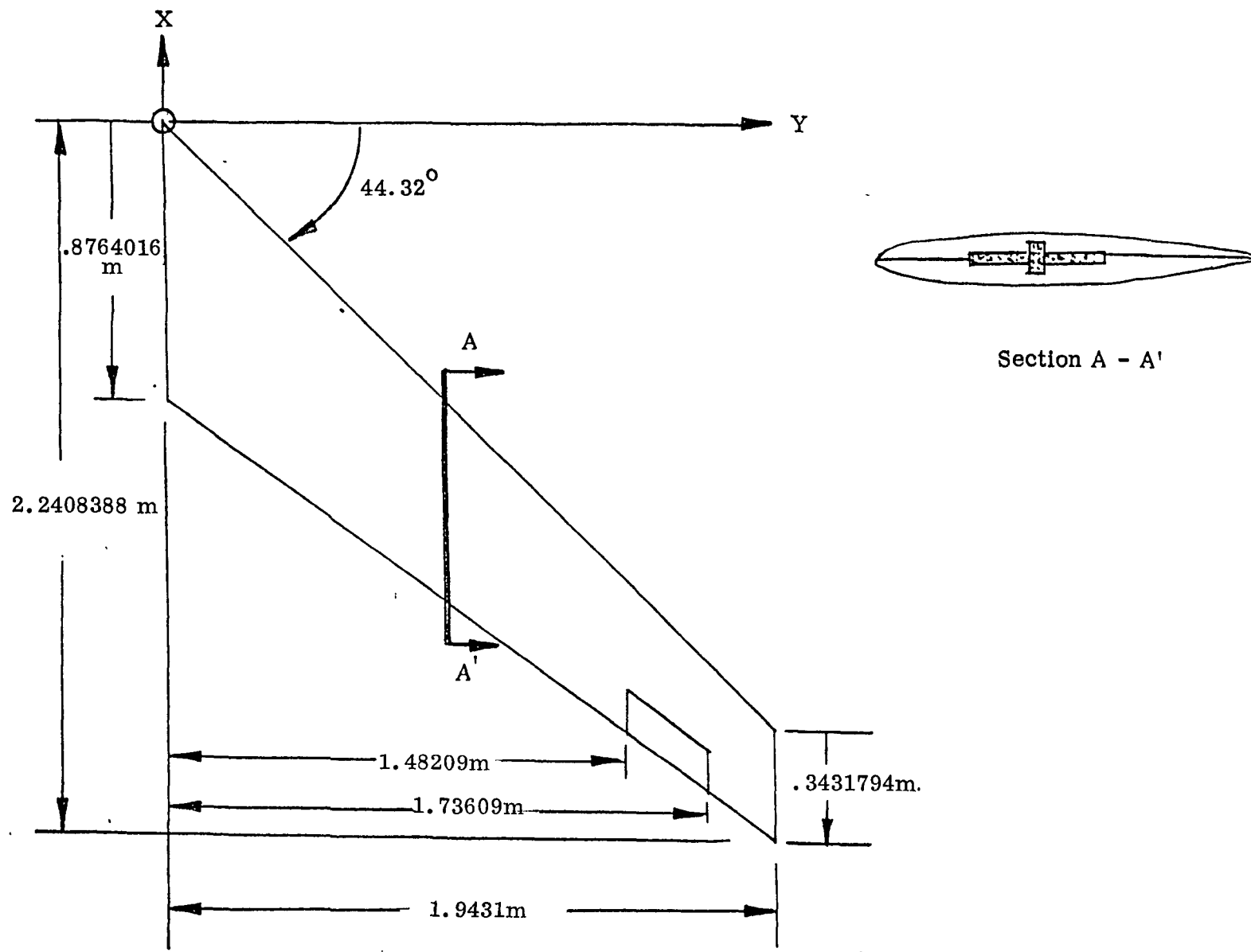
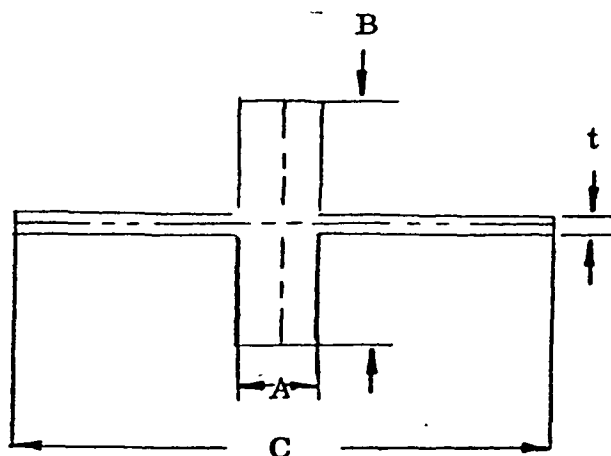


Fig. 1 Wing Planform of DAST-ARW1

TABLE 1 SPAR GEOMETRY DETAILS

DISTANCE ALONG ELASTIC AXIS METERS	A METERS	B METERS	C METERS	t METERS
0	—	—	—	—
.17145	.0331216	.0722122	.212344	.00508
.393192	.021082	.059436	.201422	.00508
.78232	.01905	.055372	.182372	.00508
1.117346	.017018	.050038	.17526	.00381
1.452118	.015748	.044196	.150368	.00381
1.787398	.014097	.03937	.128524	.00381
2.122424	.013208	.03302	.10287	.00381
2.426208	.010922	.031242	.094488	.00381



BENDING AND TORSIONAL STIFFNESS (Newton meter<sup>2</sup>)

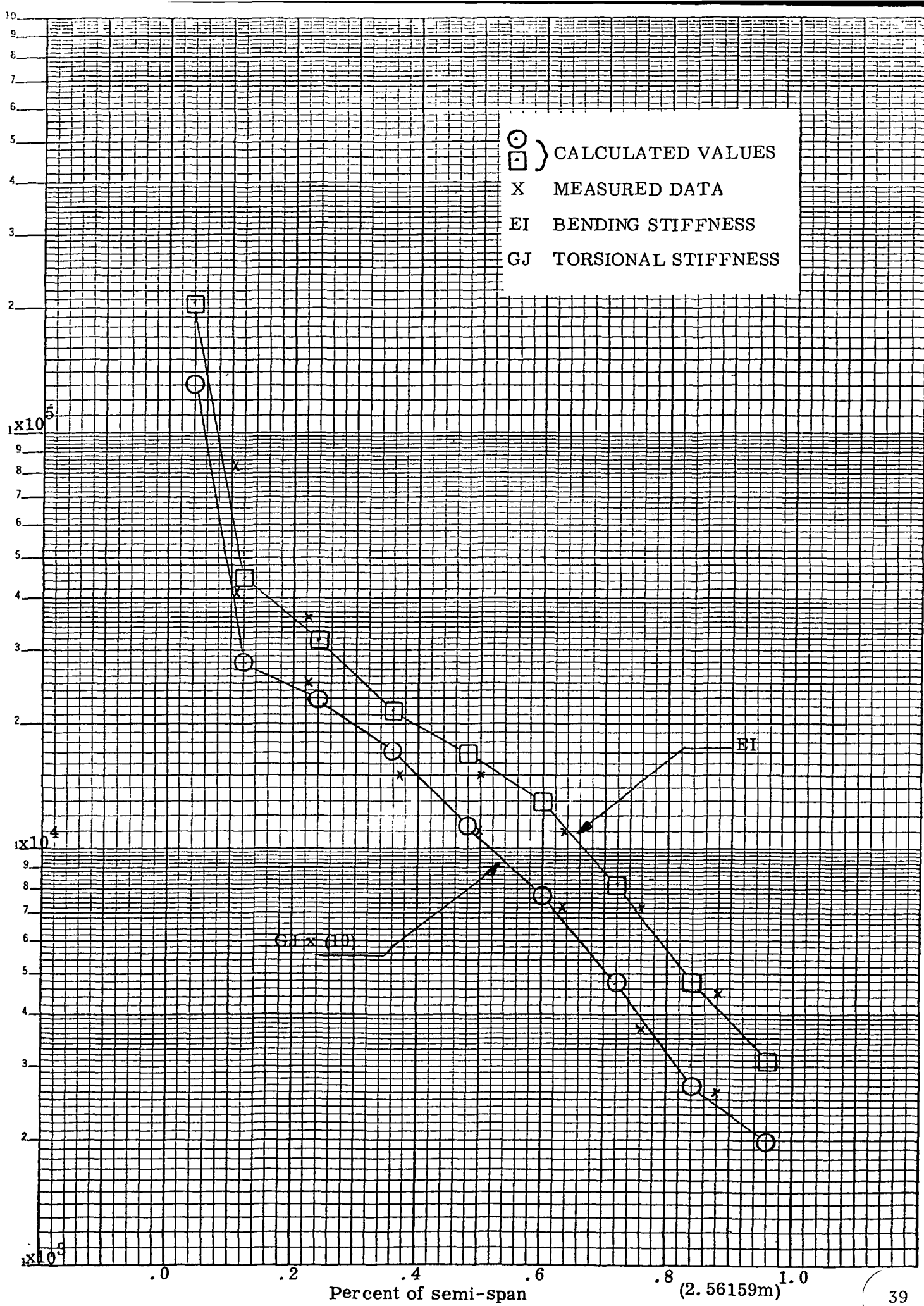


Fig. 3 Structural stiffness

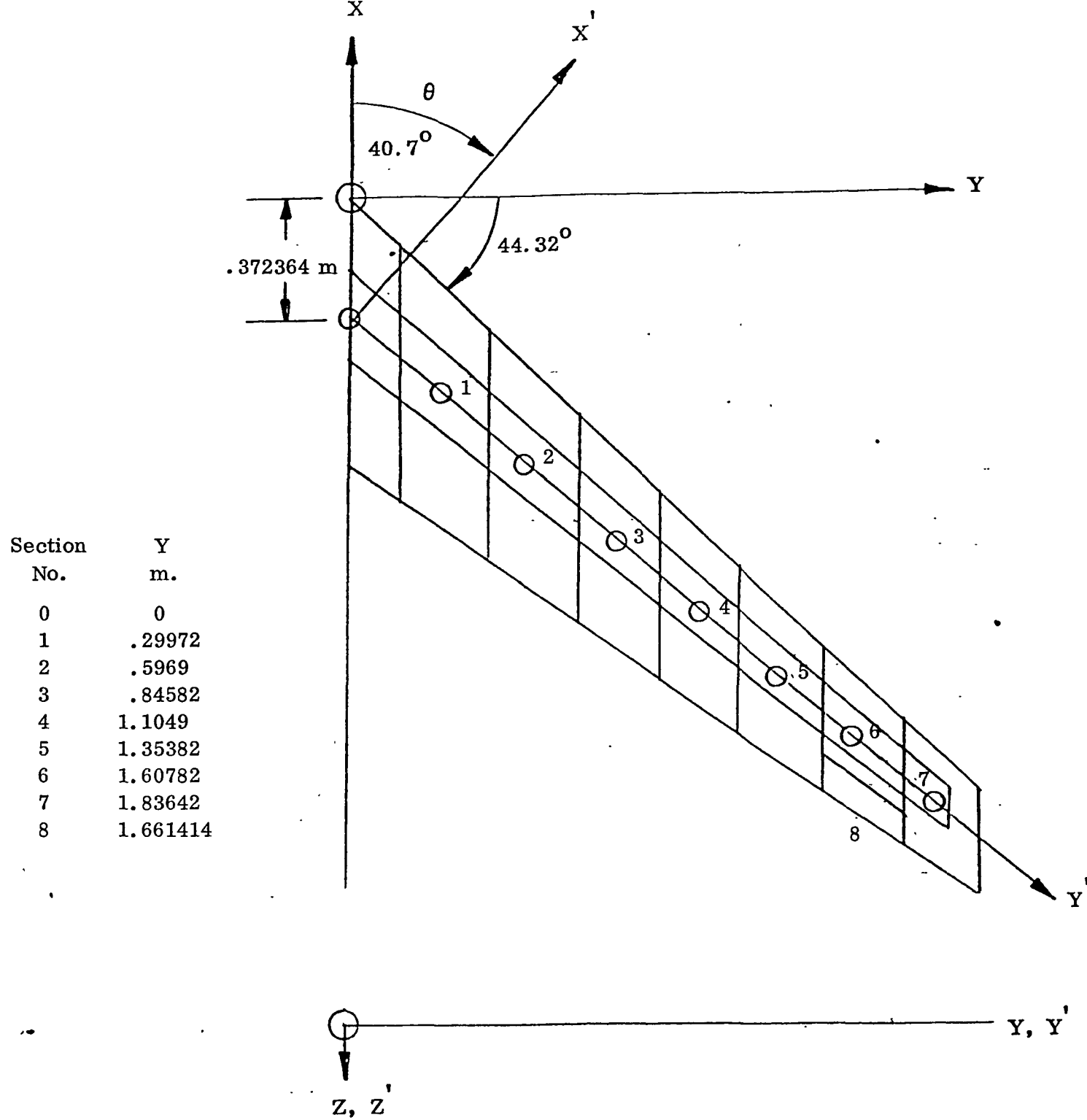


Fig. 4. Coordinate System

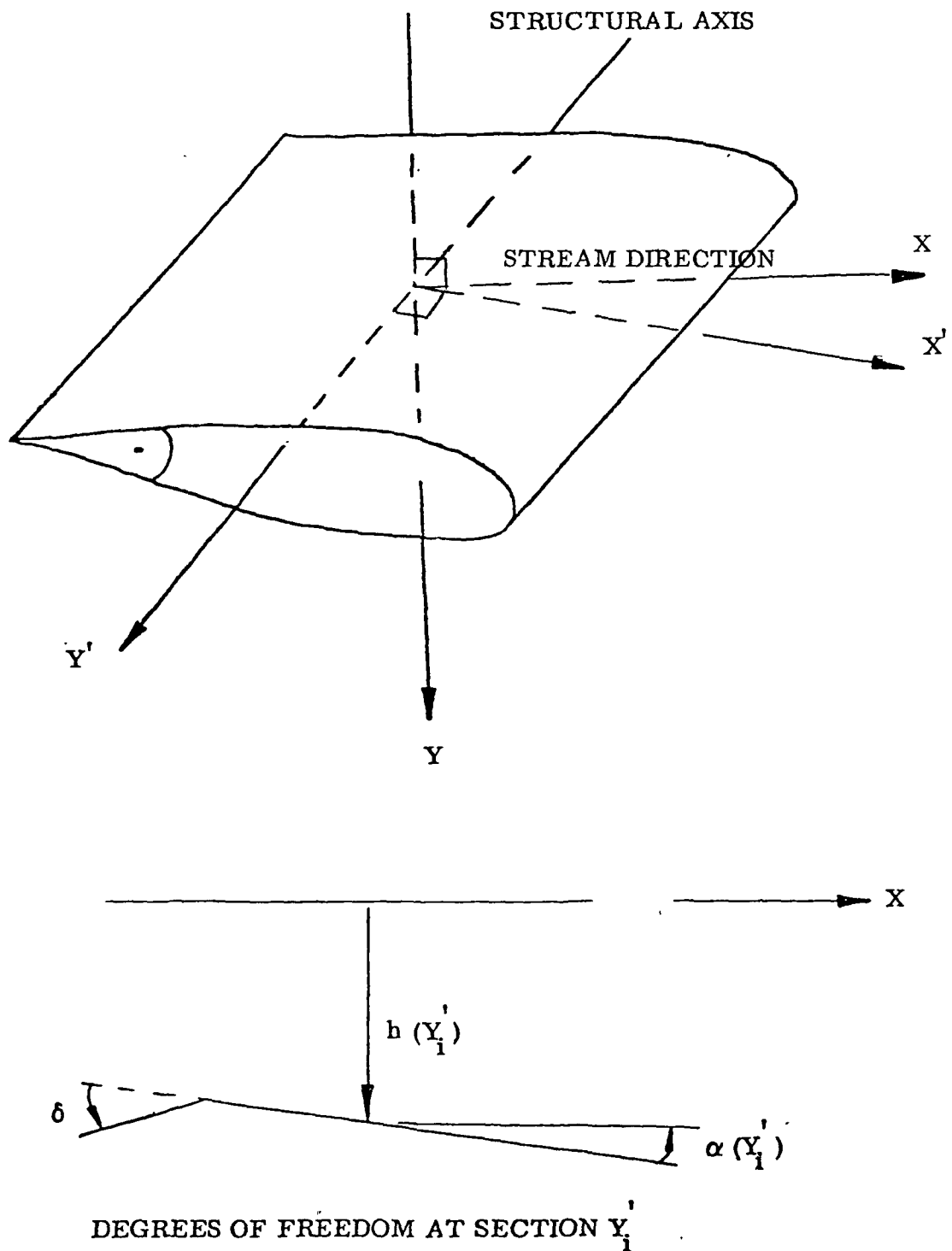


Fig. 5 Dynamical coordinate system

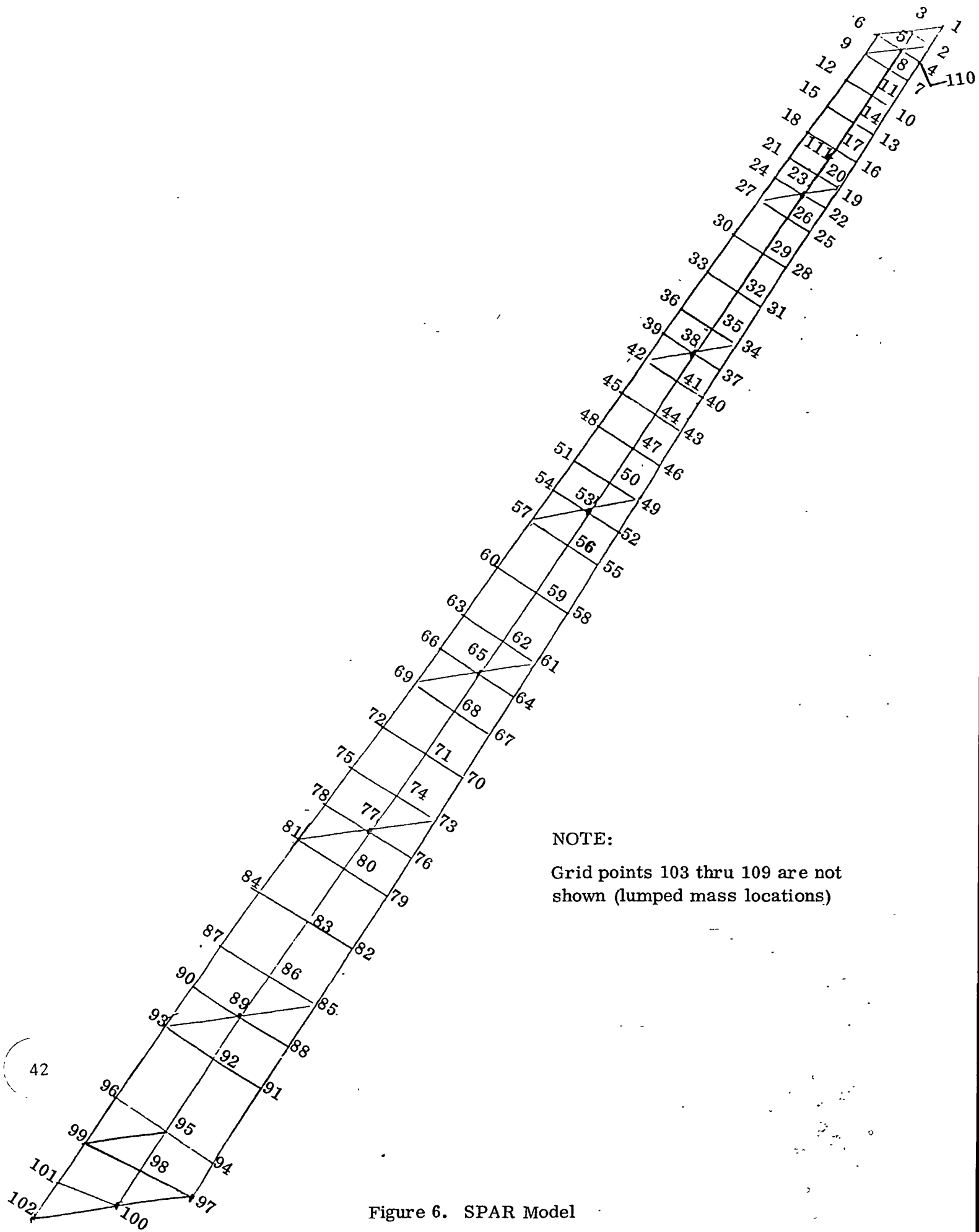
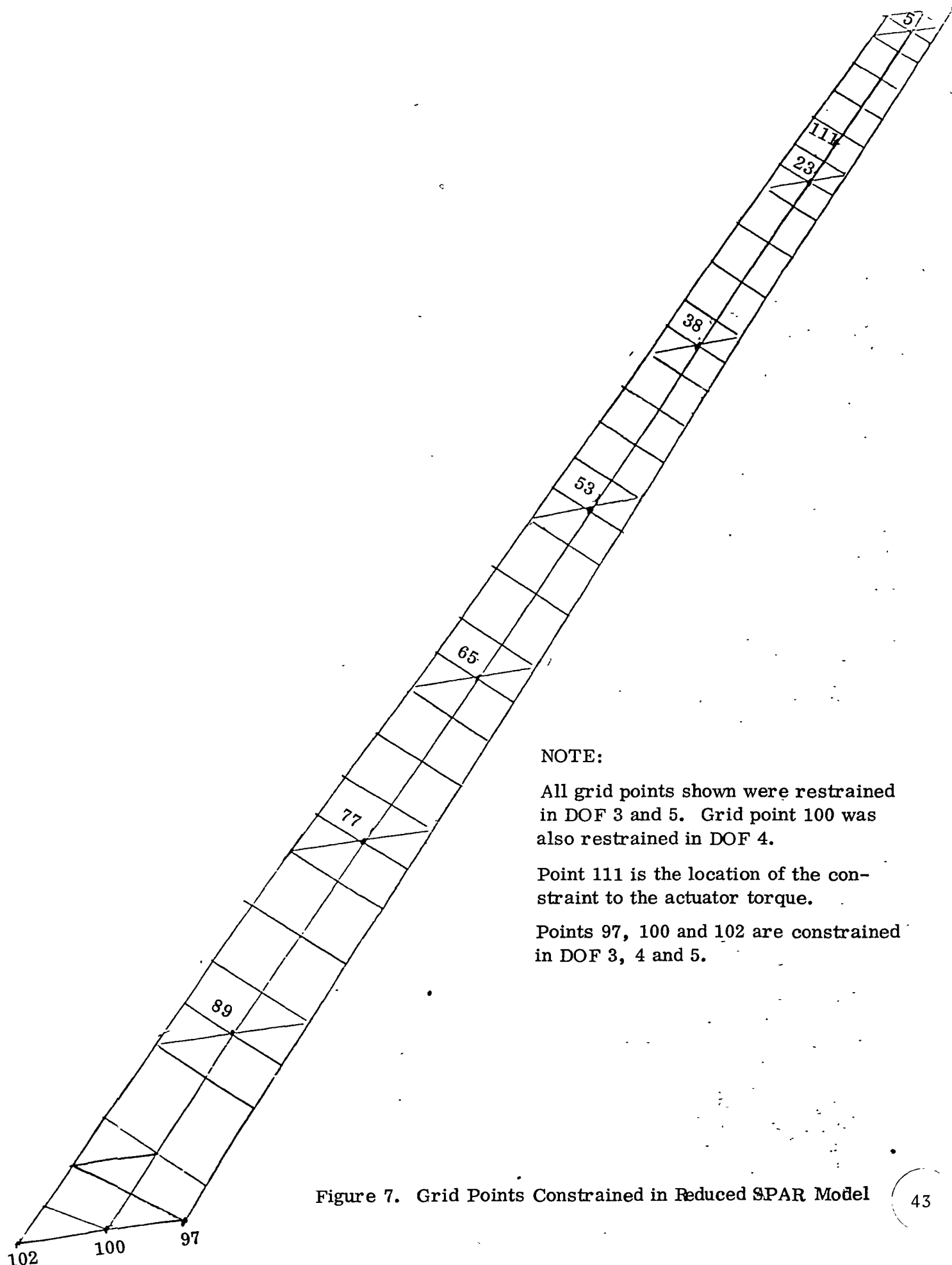


Figure 6. SPAR Model



NOTE:

All grid points shown were restrained in DOF 3 and 5. Grid point 100 was also restrained in DOF 4.

Point 111 is the location of the constraint to the actuator torque.

Points 97, 100 and 102 are constrained in DOF 3, 4 and 5.

Figure 7. Grid Points Constrained in Reduced SPAR Model

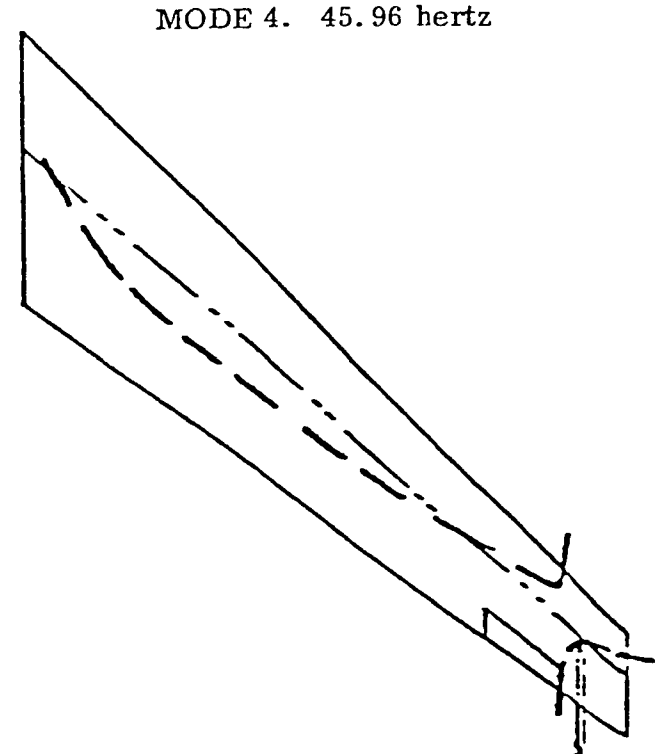
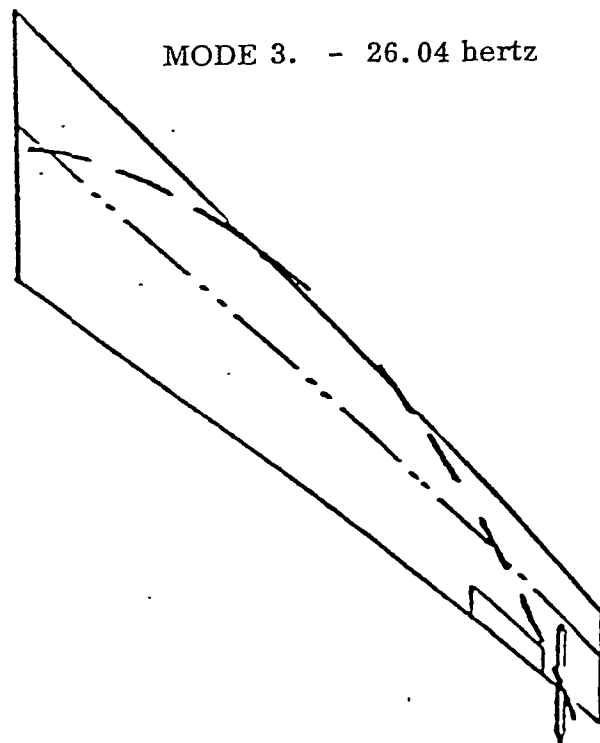
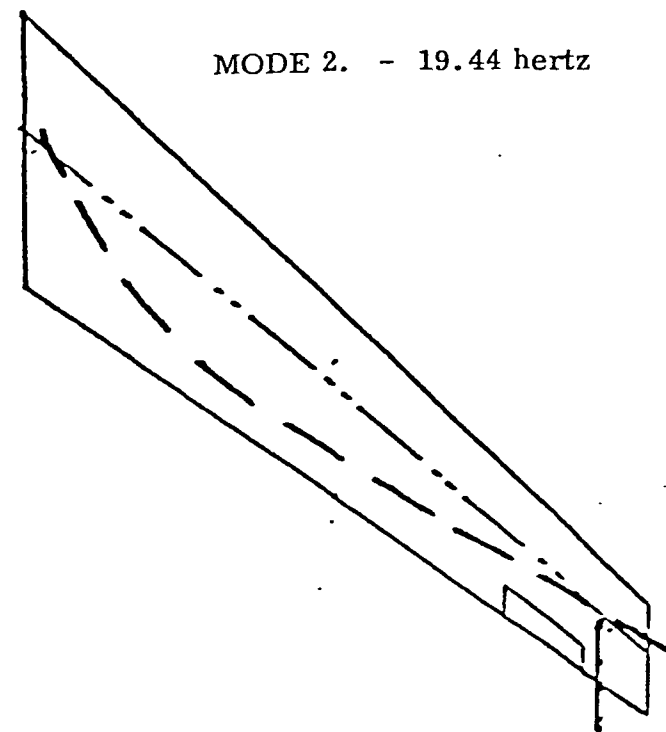
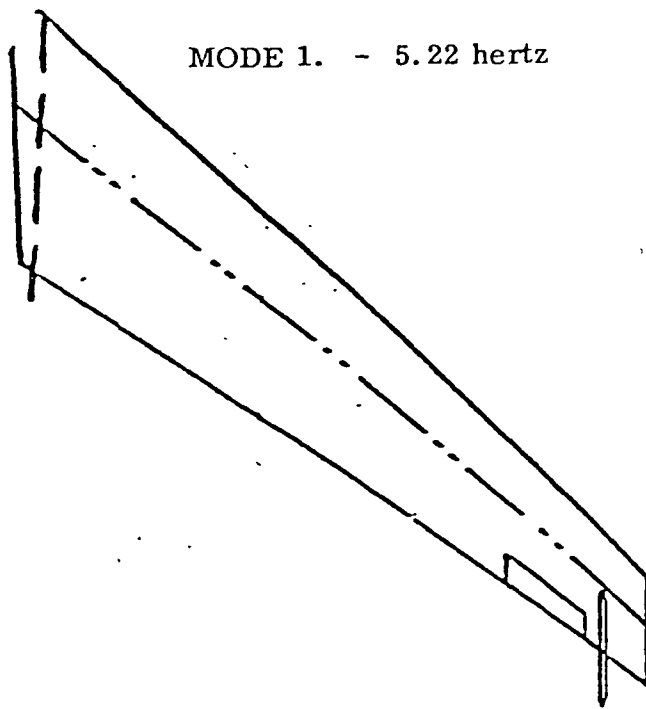
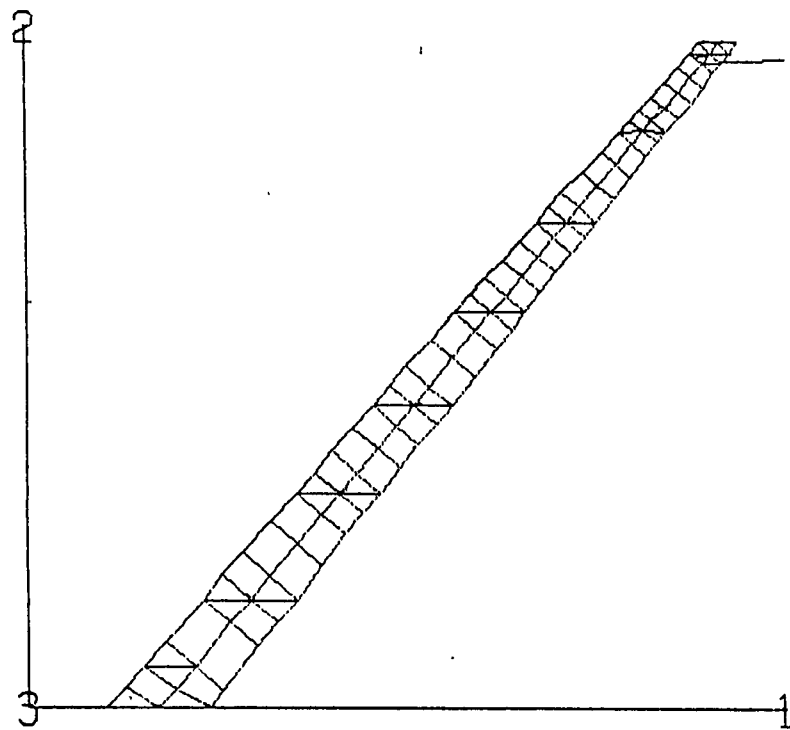


Fig. 8 Measured nodal patterns and frequencies

VIBRATIONAL MODE, FREQ (HZ)

.527873  $\times 10^{+01}$

1/1/1



SPEC  
1.1

WIND TUNNEL MODEL

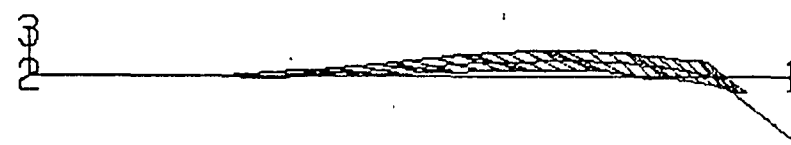
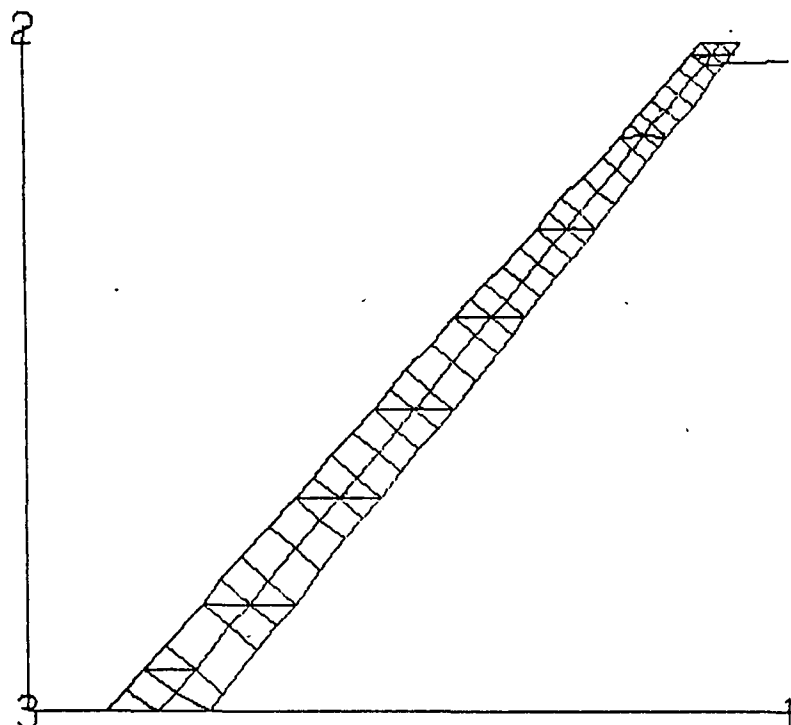
Fig. 9a Mode 1 (5 Hz)

VIBRATIONAL MODE, FREQ (HZ)

189037  $\times 10^{+02}$

1/1/3

46



SPEC  
1.1

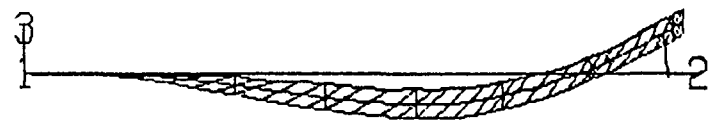
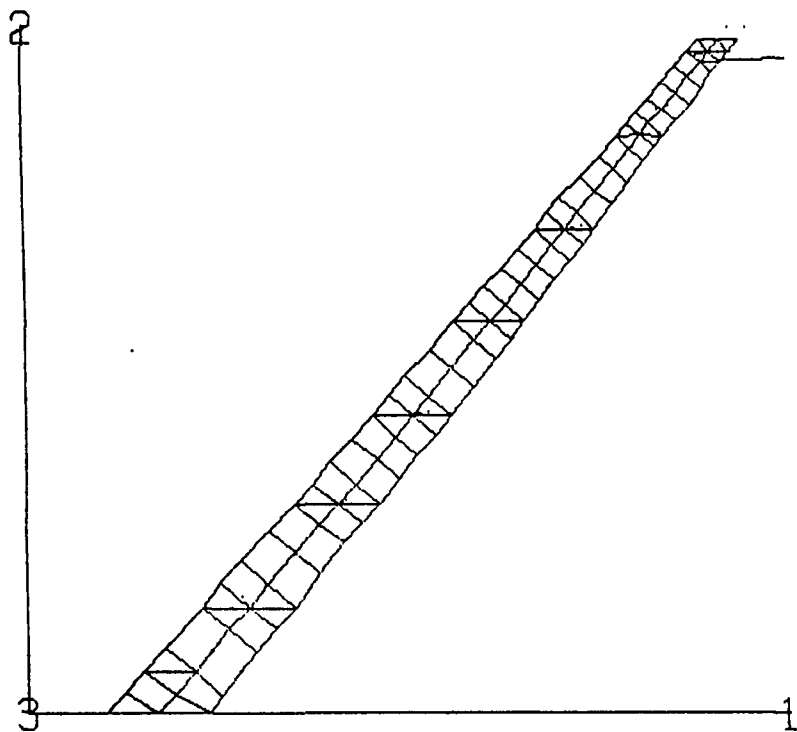
WIND TUNNEL MODEL

Fig. 9b Mode 2 (19 Hz)

VIBRATIONAL MODE, FREQ (HZ)

260087 X10<sup>+02</sup>

1 / 1 / 4



SPEC  
1.1

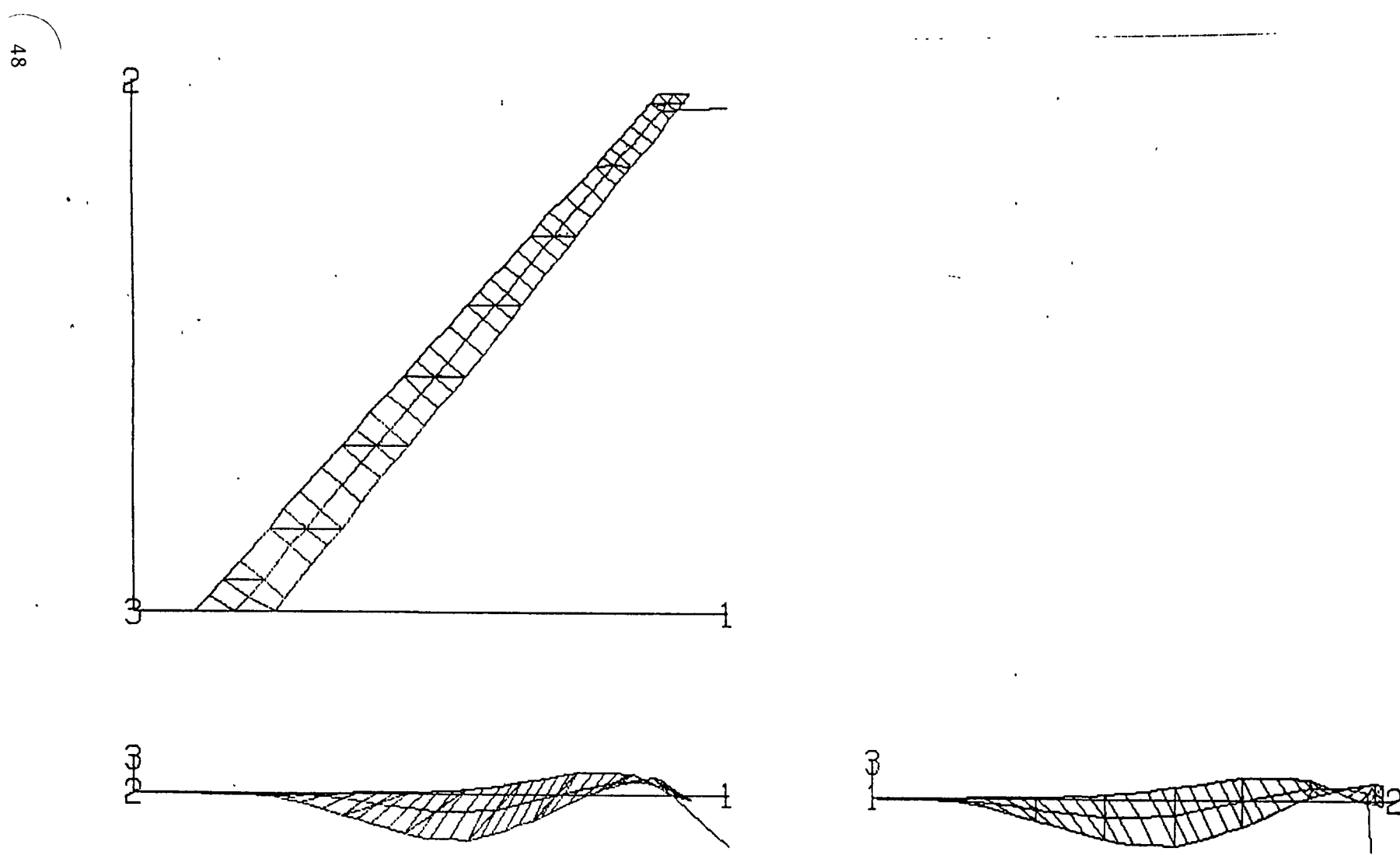
WIND TUNNEL MODEL

Fig. 9c Mode 3 (26 Hz)

VIBRATIONAL MODE, FREQ (HZ)

.443395 X10 +02

1 / 1 / 5



SPEC  
1.1

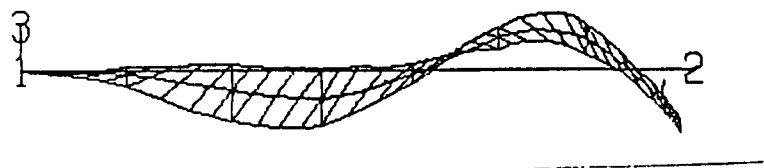
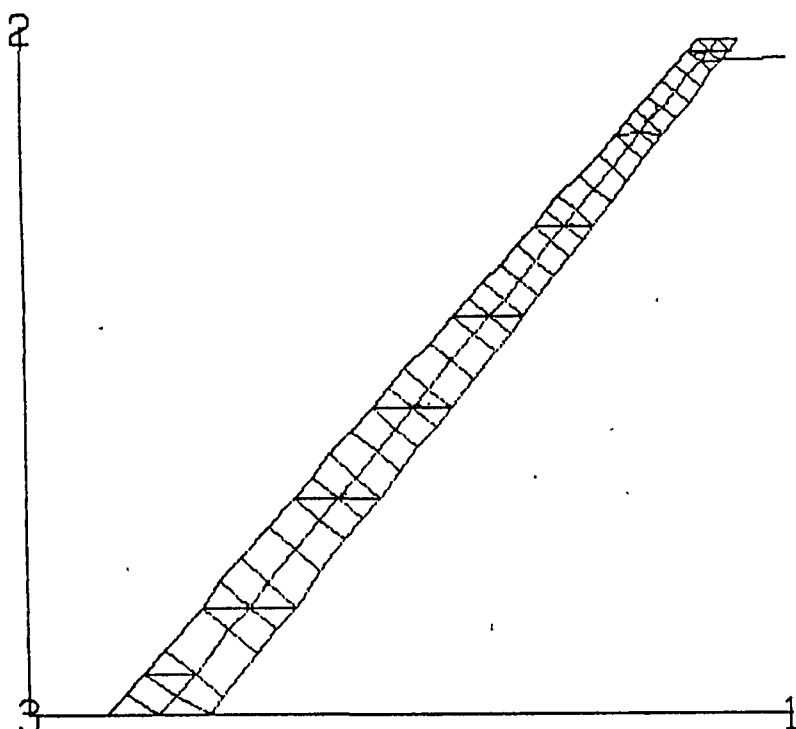
WIND TUNNEL MODEL

Fig. 9d Mode 4 (44 Hz)

VIBRATIONAL MODE, FREQ (HZ)

• 601990 X10<sup>+02</sup>

1/1/7



SPEC  
1.1

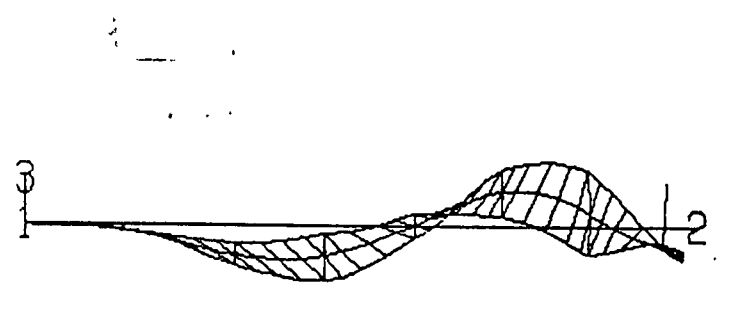
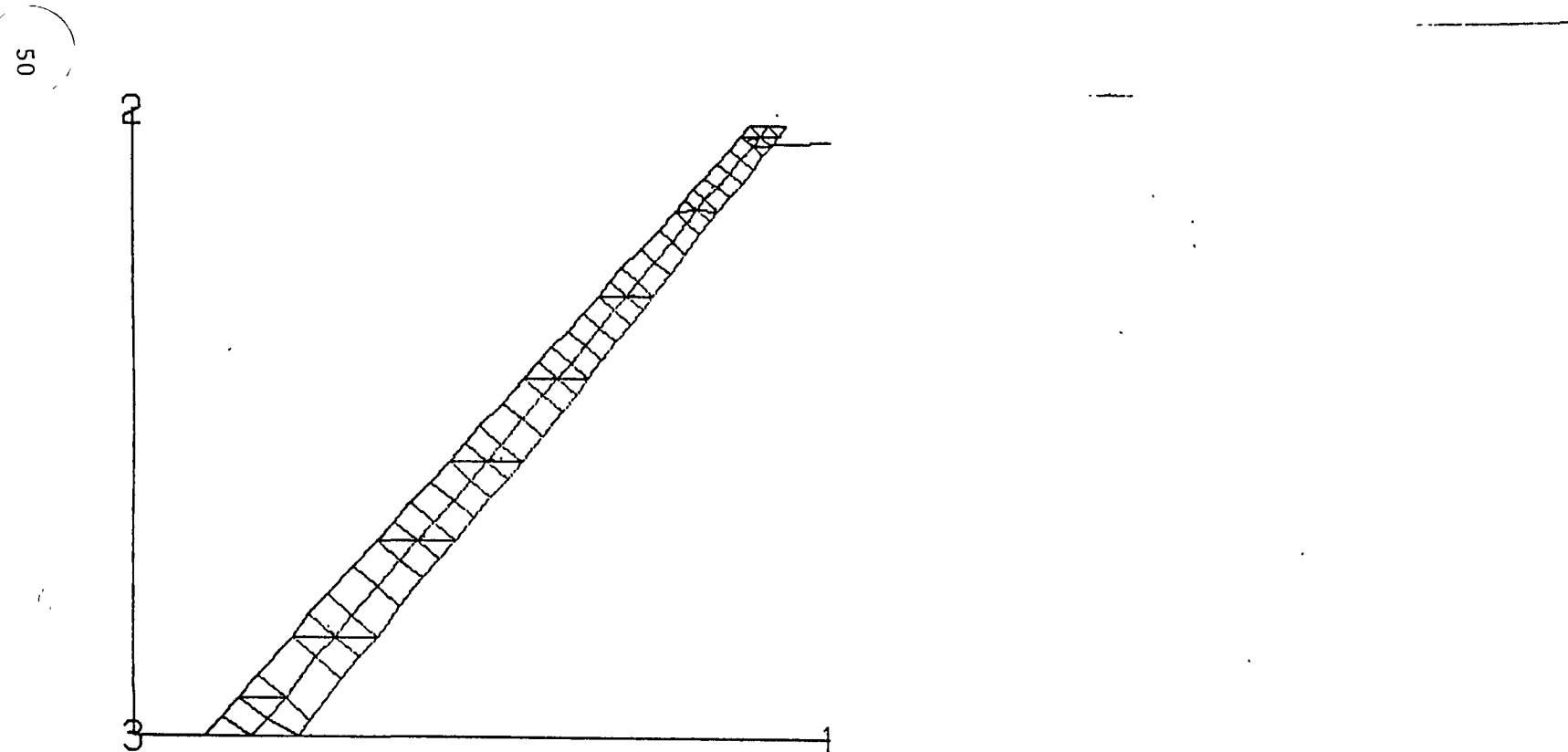
WIND TUNNEL MODEL

Fig. 10 Mode 5 (60 Hz)

VIBRATIONAL MODE, FREQ (HZ)

.738675 X10<sup>+02</sup>

1/1/87



SPEC  
1.1

WIND TUNNEL MODEL

Fig. 11 Mode 6 (74 Hz)

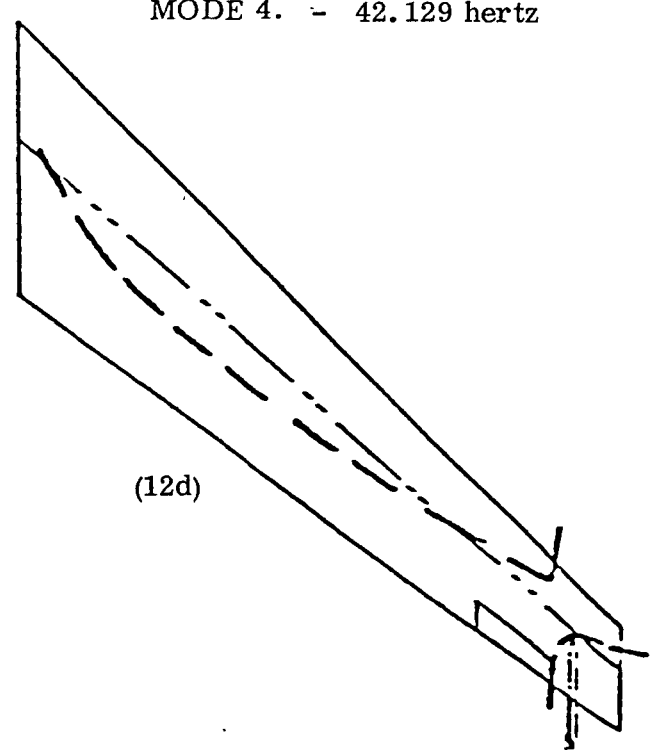
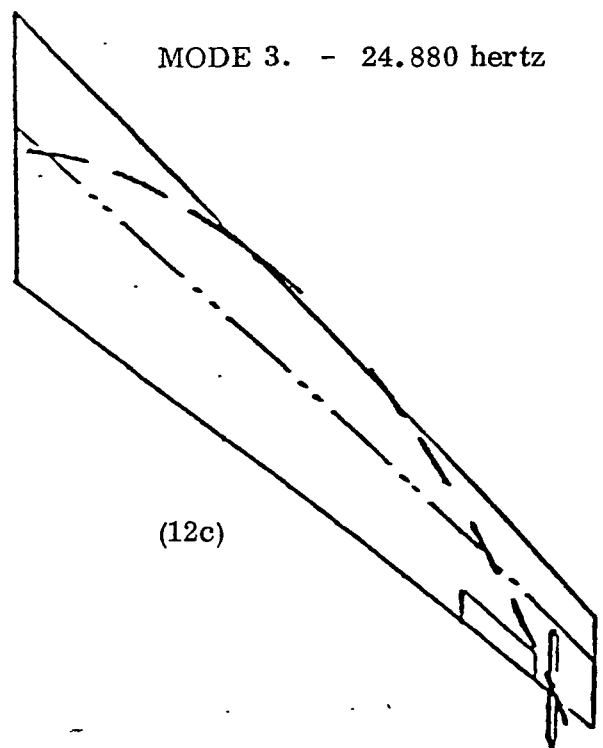
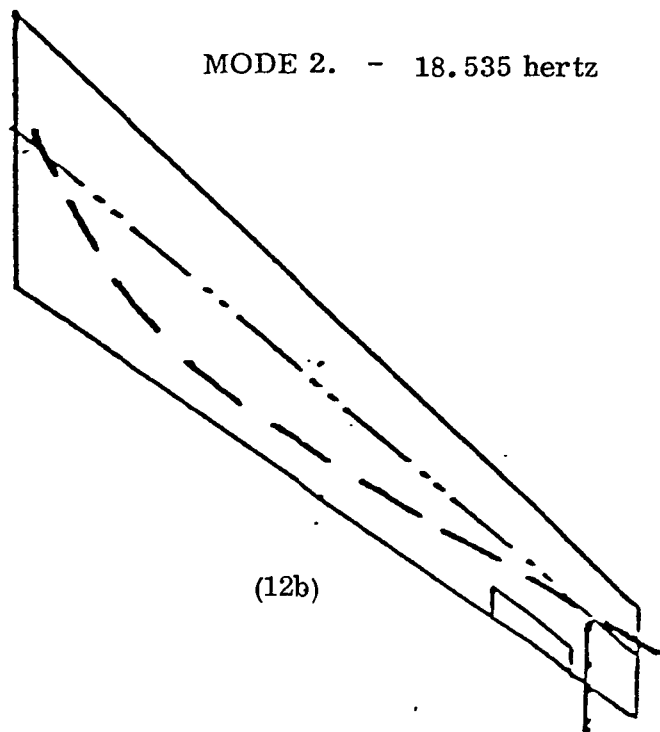
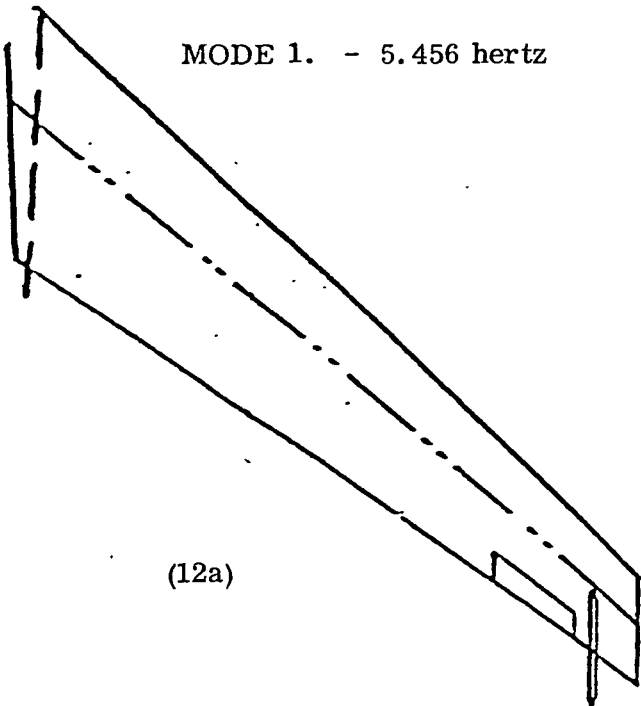


Fig. 12 First Four Normal Modes of Reduced Dynamical System at  
Zero Airspeed

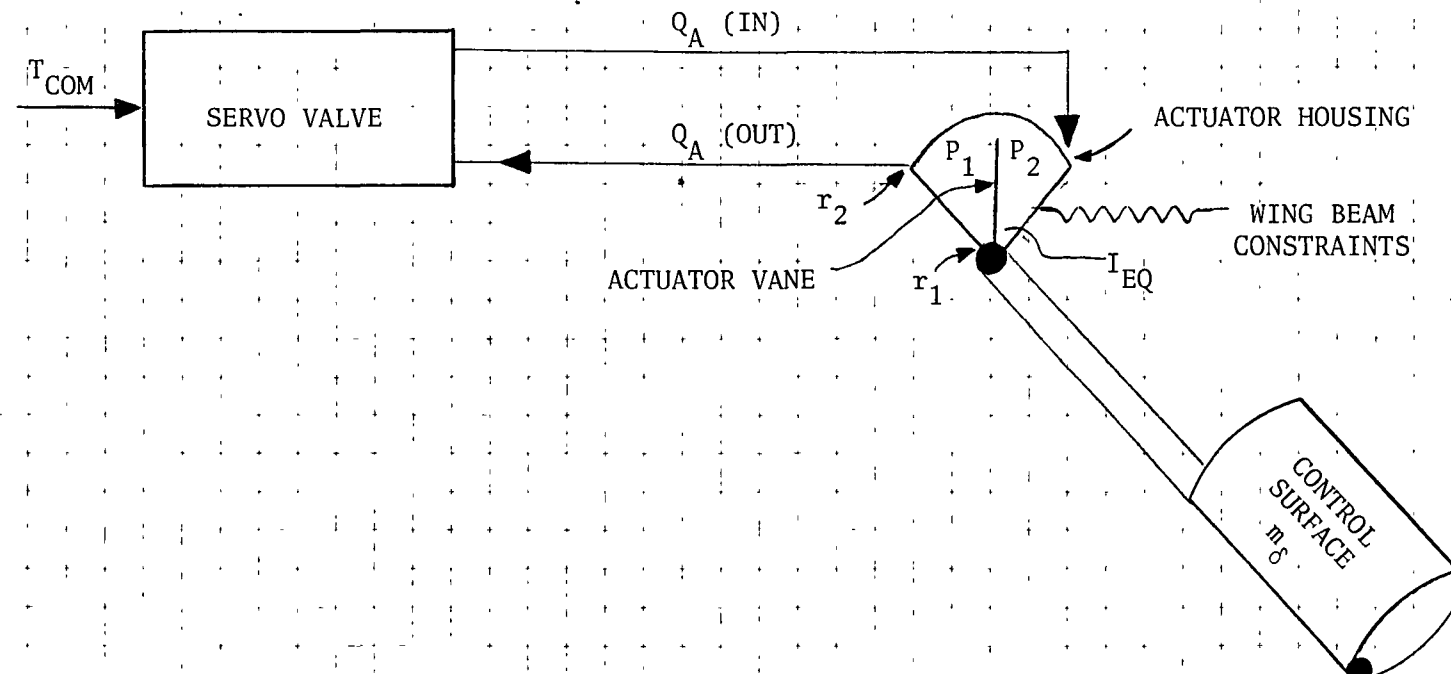


Figure 13. Actuator

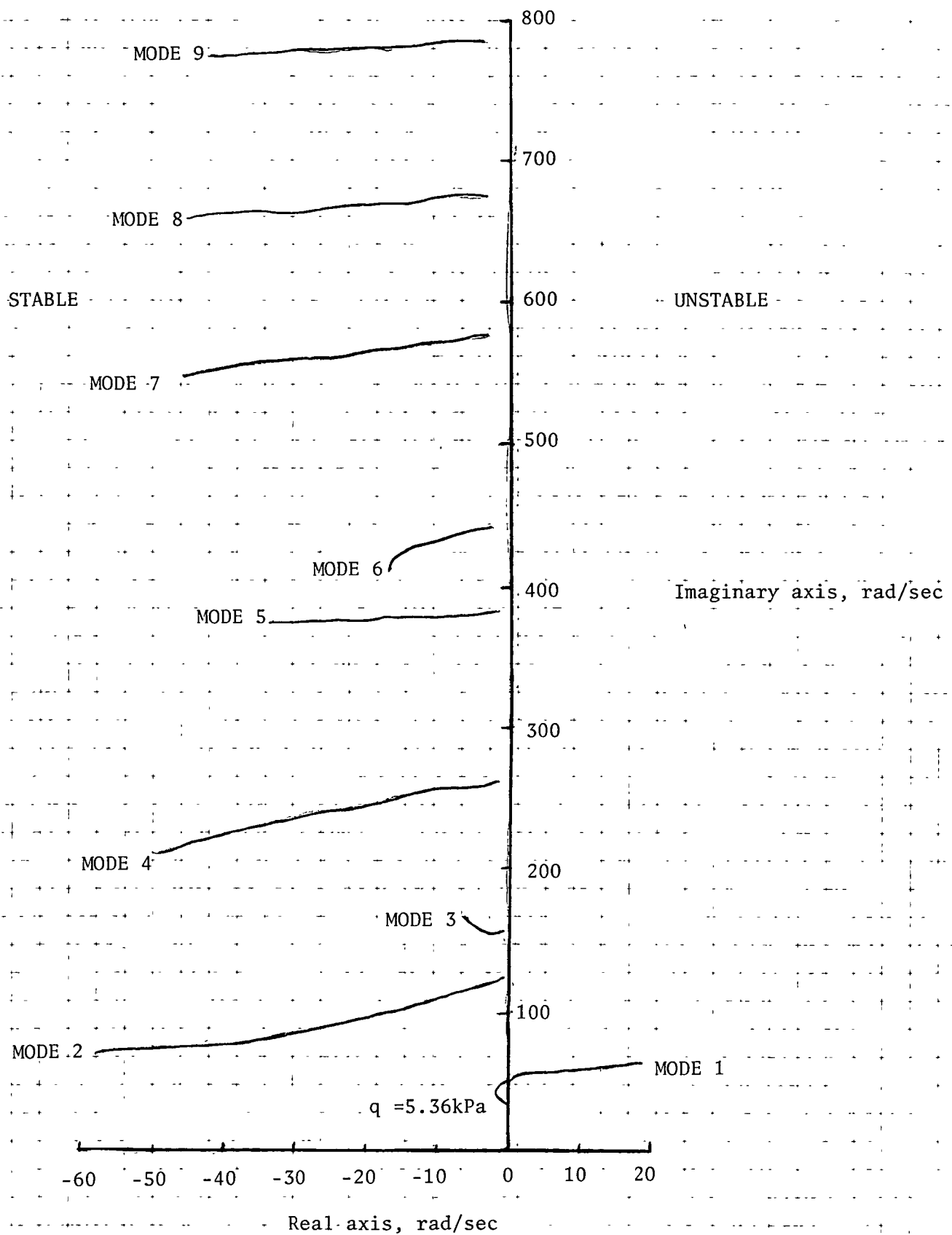


Figure 14. Open loop eigenvalues of flexible modes as a function of dynamic pressure.

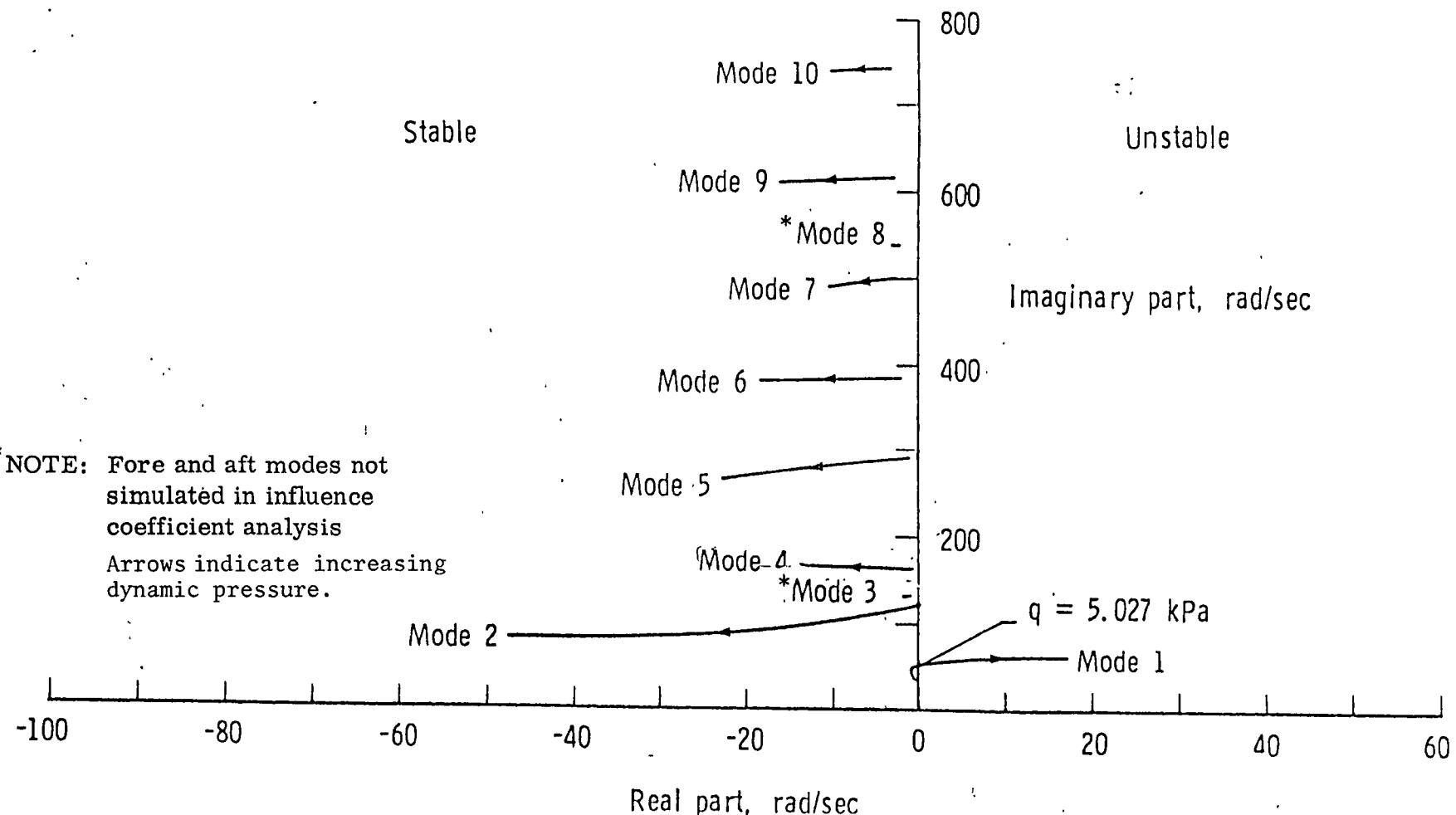


Figure 15. Dynamic-pressure root locus at  $M = 0.90$  (system off), (Ref. 1).

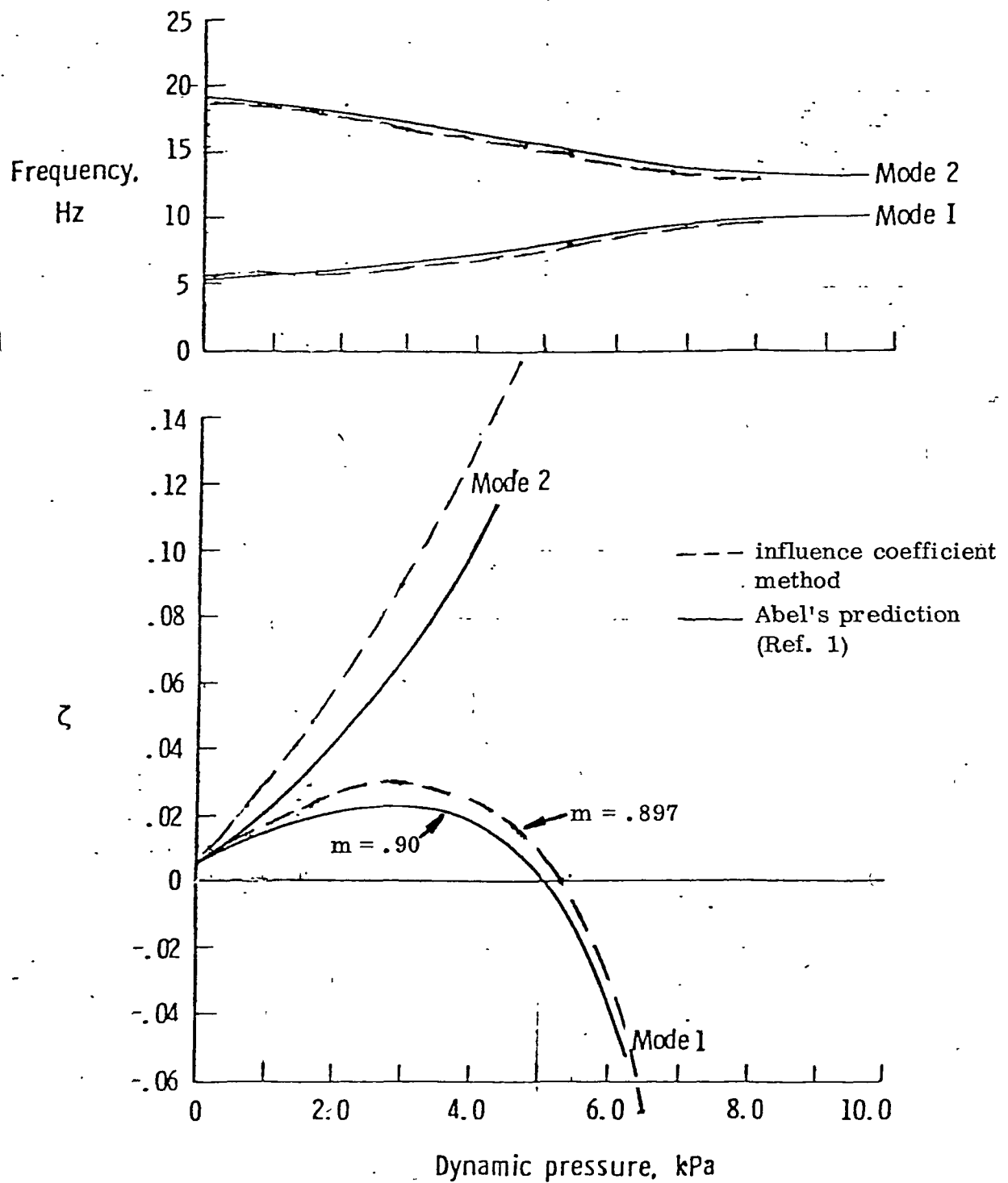


Figure 16. Damping and frequency versus dynamic pressure (system off).

TABLE 2. MATRIX OF INFLUENCE COEFFICIENTS.

ROW	COL 1	COL 2	COL 3	COL 4	COL 5
1	.22677542000000E+08	-.70437274000000E+07	.23725273000000E+07	-.45362964000000E+06	.91084763000000E+05
2	-.70437274000000E+07	.66060031000000E+07	-.43556373000000E+07	.14240211000000E+07	-.28590647000000E+06
3	.23725273000000E+07	-.43556373000000E+07	.50189197000000E+07	-.29510165000000E+07	.96107681000000E+06
4	-.45362964000000E+06	.14240211000000E+07	-.29610165000000E+07	.32685585000000E+07	-.19638215000000E+07
5	.91084763000000E+05	-.28590647000000E+06	.96107681000000E+06	-.19638215000000E+07	.21367190000000E+07
6	-.16839310000000E+05	.52857009000000E+05	-.17766758000000E+06	.59815586000000E+06	-.11624155000000E+07
7	.22799027000000E+04	-.71563987000000E+04	.24054704000000E+05	-.80980505000000E+05	.25714119000000E+06
8	-.25493803000000E+06	-.14130021000000E+05	.19684573000000E+05	-.37508881000000E+04	.75314709000000E+03
9	.92075518000000E+05	-.10978278000000E+05	-.35865855000000E+05	.22395328000000E+05	-.44931531000000E+04
10	-.33282973000000E+05	.39530705000000E+05	-.95780175000000E+04	-.20967253000000E+05	.14092687000000E+05
11	.553158386000000E+04	-.17384829000000E+05	.20227640000000E+05	.58242167000000E+04	-.21338244000000E+05
12	-.14706408000000E+04	.46161998000000E+04	-.15525392000000E+05	.22592046000000E+05	-.84179747000000E+04
13	.48248703000000E+03	-.15144816000000E+04	.50906071000000E+04	-.17144015000000E+05	.33944755000000E+05
14	-.29403225000000E+02	.92293970000000E+02	-.31022640000000E+03	.10443819000000E+04	-.33160655000000E+04
15	-.13415067000000E+03	.42108641000000E+03	-.14153916000000E+04	.47649394000000E+04	-.15134340000000E+05
16	0.	0.	0.	0.	0.

ROW	COL 6	COL 7	COL 8	COL 9	COL 10
1	-.16839310000000E+05	.22799027000000E+04	-.25493803000000E+06	.92075518000000E+05	-.33282973000000E+05
2	.52857009000000E+05	-.71563987000000E+04	-.14130021000000E+05	-.10978278000000E+05	.39630705000000E+05
3	-.17766758000000E+06	.24054704000000E+05	.19684573000000E+05	-.35965855000000E+05	-.95780175000000E+04
4	.59815586000000E+06	-.80980505000000E+05	-.37508881000000E+04	.22395328000000E+05	-.20967253000000E+05
5	-.11624155000000E+07	.25714118000000E+06	.75314708000000E+03	-.44931531000000E+04	.14092687000000E+05
6	.10968903000000E+07	-.39724283000000E+06	-.13923819000000E+03	.83067291000000E+03	-.26035997000000E+04
7	-.39724283000000E+06	.20275204000000E+06	.18851692000000E+02	-.11246621000000E+03	.35250564000000E+03
8	-.13923819000000E+03	.18851692000000E+02	.70244589000000E+05	-.13881949000000E+05	-.28450619000000E+03
9	.83067291000000E+03	-.11246621000000E+03	-.13881949000000E+05	.25591945000000E+05	-.11007806000000E+05
10	-.26035997000000E+04	.35250564000000E+03	-.28450619000000E+03	-.11007806000000E+05	.18482635200000E+05
11	.10635177000000E+05	-.14394196000000E+04	-.45739750000000E+02	-.27482012000000E+03	-.70618411000000E+04
12	-.58111389000000E+04	.34699416000000E+04	-.12160196000000E+02	.72546282000000E+02	-.22810394000000E+03
13	-.82601118000000E+04	-.12419799000000E+05	.39895124000000E+01	-.23800797000000E+02	.74599645000000E+02
14	.10553793000000E+05	-.80457075000000E+04	-.24312471000000E+00	.14504439000000E+01	-.45461615000000E+01
15	-.22129004000000E+04	.13660862000000E+05	-.11092438000000E+01	.66175723000000E+01	-.20741619000000E+02
16	0.	0.	0.	0.	0.

TABLE 2. (CONCLUDED).

ROW	COL 11	COL 12	COL 13	COL 14	COL 15
1	.55316838000000E+04	-.14706408000000E+04	.48248703000000E+03	-.29403225000000E+02	-.13415057000000E+03
2	-.17384829000000E+05	.46161998000000E+04	-.15144816000000E+04	.92293970000000E+02	.42108641000000E+03
3	.20228764000000E+05	-.15525392000000E+05	.50906071000000F+04	-.31022640000000E+03	-.14153915000000E+04
4	.58242167000000E+04	.22592046000000E+05	-.17144015000000E+05	.10443819000000E+04	.47649394000000E+04
5	-.21338244000000E+05	-.84179747000000E+04	.33944766000000E+05	-.33160665000000E+04	-.15134340000000E+05
6	.10635177000000E+05	-.58111389000000E+04	-.82601118000000E+04	.10553793000000E+05	-.22129004000000F+04
7	-.14394196000000E+04	.34699416000000E+04	-.12419799000000E+05	-.80457075000000E+04	.13660852000000F+05
8	.45739750000000E+02	-.12160196000000E+02	.39895124000000F+01	-.24312471000000E+00	-.11092439000000E+01
9	-.27482012000000E+03	.72546282000000F+02	-.23800797000000F+02	.14504439000000E+01	.66175723000000F+01
10	-.70618411000000E+04	-.22810394000000E+03	.74599646000000F+02	-.45461615000000E+01	-.20741619000000E+02
11	.12223524000000E+05	-.47593176000000E+04	-.30498356000000F+03	.18563780000000E+02	.84696399000000E+02
12	-.47593176000000E+04	.82452498000000E+04	-.28966418000000F+04	-.44656372000000E+02	-.20315192000000E+03
13	-.30498356000000E+03	-.28966418000000E+04	.14688000000000E+05	-.33430934000000E+02	-.85251810000000E+04
14	.18563780000000E+02	-.44656372000000E+02	-.33430934000000E+02	.28029254000000E+04	-.20801117000000E+04
15	.84696399000000E+02	-.20315192000000E+03	-.85251810000000E+04	-.20801117000000E+04	.81689105000000E+04
16	0.	0.	0.	0.	-.19887815000000E+02
ROW	COL 16				
1	0.				
2	0.				
3	0.				
4	0.				
5	0.				
6	0.				
7	0.				
8	0.				
9	0.				
10	0.				
11	0.				
12	0.				
13	0.				
14	0.				
15	-.19887816000000E+02				
16	.19887816000000E+02				

TABLE 3  
COMBINED BEAM AND PLATE ELEMENT MASS PROPERTIES

Section No.	Mass (kgm)	$I_Y'$ (kgm $\cdot$ m $^2$ )	$I_X'$ (kgm $\cdot$ m $^2$ )	$I_{Z'}=I_Z$ (kgm $\cdot$ m $^2$ )	$I_X$ (kgm $\cdot$ m $^2$ )	$I_Y$ (kgm $\cdot$ m $^2$ )
0*	7.1088	.0262	.0654	.0913	.0487	.0429
1	2.5310	.0048	.0343	.0382	.0218	.0173
2	1.8328	.0026	.0199	.0220	.0126	.0100
3	1.3659	.0017	.0128	.0142	.0081	.0064
4	1.1339	.0012	.0107	.0116	.0066	.0052
5	.9982	.0010	.0095	.0103	.0059	.0046
6	.7266	.0002	.0058	.0061	.0034	.0026
7	.3341	.0001	.0023	.0024	.0014	.0011

---

16.0313

\* Wing root section mass properties

\*\* Compares with 15.8773 kgm calculated by SPAR

TABLE 4  
CONCENTRATED MASS PROPERTIES IN X-Y COORDINATE SYSTEM

Section No.	Mass (kgm)	Pitch Inertia $I_Y$ ( $\text{kgm} \cdot \text{m}^2$ )	Yaw Inertia $I_Z$ ( $\text{kgm} \cdot \text{m}^2$ )	Roll Inertia $I_X$ ( $\text{kgm} \cdot \text{m}^2$ )	$\Delta X^{**}$ (m)	$\Delta Y^{**}$ (m)	Pitch Inertia $I_Y(\text{grid point})$ ( $\text{kgm} \cdot \text{m}^2$ )
1	1.6556	.0734	.0801	.0134	-.0051	+.0152	.0734
2	1.0342	.0430	.0443	.0044	+.0147	+.0053	.0432
3	1.1975 *	.0333	.0344	.0042	+.0239	+.0036	.0340
4	1.1612 *	.0267	.0280	.0034	.0201	.0028	.0272
5	1.0161	.0177	.0192	.0027	.0218	.0041	.0182
6	1.4198	.0200	.0206	.0047	.0285	.0000	.0211
7***	.6350	.0101	.0127	.0021	-.0521	-.0112	.0118
7***	.5534	.0056	0	.0056	.2070	-.0210	.0293
7***	.4627	0	0	0	0	0	0
<hr/>							
9.1355							

$$I_{Y(\text{grid point})} = I_Y + m \Delta X^2$$

\* These values were altered to agree with SPAR computer model

\*\*  $\Delta X$  - Mass offset from grid point in X direction

$\Delta Y$  - Mass offset from grid point in Y direction

\*\*\* These masses were added to cause flutter within the available wind tunnel dynamic pressure.

TABLE 5. MASS MATRIX.

ROW	COL 1	COL 2	COL 3	COL 4	COL 5
1	.41866697000000E+01	0.	0.	0.	0.
2	0.	.28671590000000E+01	0.	0.	0.
3	0.	0.	.25632614000000E+01	0.	0.
4	0.	0.	0.	.22951773000000E+01	0.
5	0.	0.	0.	0.	.20144139000000E+01
6	0.	0.	0.	0.	0.
7	0.	0.	0.	0.	0.
8	0.	0.	0.	0.	0.
9	0.	0.	0.	0.	0.
10	0.	0.	0.	0.	0.
11	0.	0.	0.	0.	0.
12	0.	0.	0.	0.	0.
13	0.	0.	0.	0.	0.
14	0.	0.	0.	0.	0.
15	0.	0.	0.	0.	0.
16	0.	0.	0.	0.	0.

ROW	COL 6	COL 7	COL 8	COL 9	COL 10
1	0.	0.	0.	0.	0.
2	0.	0.	0.	0.	0.
3	0.	0.	0.	0.	0.
4	0.	0.	0.	0.	0.
5	0.	0.	0.	0.	0.
6	.21464070000000E+01	0.	0.	0.	0.
7	0.	.19853779000000E+01	0.	0.	0.
8	0.	0.	.90750036000000E-01	0.	0.
9	0.	0.	0.	.53153973000000E-01	0.
10	0.	0.	0.	0.	.40454275000000E-01
11	0.	0.	0.	0.	0.
12	0.	0.	0.	0.	0.
13	0.	0.	0.	0.	0.
14	0.	0.	0.	0.	0.
15	0.	0.	0.	0.	0.
16	0.	0.	0.	0.	0.

TABLE 5. (CONCLUDED).

ROW	COL 11	COL 12	COL 13	COL 14	COL 15
1	0.	0.	0.	0.	0.
2	0.	0.	0.	0.	0.
3	0.	0.	0.	0.	0.
4	0.	0.	0.	0.	0.
5	0.	0.	0.	0.	0.
6	0.	0.	0.	0.	0.
7	0.	0.	0.	0.	0.
8	0.	0.	0.	0.	0.
9	0.	0.	0.	0.	0.
10	0.	0.	0.	0.	0.
11	.32363657000000E-01	0.	0.	0.	0.
12	0.	.22762138000000E-01	0.	0.	0.
13	0.	0.	.23737502000000E-01	0.	0.
14	0.	0.	0.	.42146030000000E-01	0.
15	0.	0.	0.	0.	.26229429000000E-03
16	0.	0.	0.	0.	0.

ROW	COL 16
1	0.
2	0.
3	0.
4	0.
5	0.
6	0.
7	0.
8	0.
9	0.
10	0.
11	0.
12	0.
13	0.
14	0.
15	0.
16	.22097573000000E-03

TABLE 6  
COMPARISON OF VIBRATION MODES

	Vibration Test Freq.	(Hz) SPAR 666 DOF	Reduced Model 16 DOF
1	5.22	5.279	5.432
2	19.44	18.90	17.532
3	26.04	26.01	24.76
4	45.96	44.34	41.38
5	N/A	60.19	45.73
6		73.87	60.64
7		84.96	68.85
8		93.18	91.34
9			107.29
10			125.08
11			135.51
12			147.18
13			203.88
14			296.70
15			420.03
16			894.13

TABLE 7.  $H_1$  MATRIX.

ROW	COL 1	COL 2	COL 3	COL 4	COL 5
1	0.	0.	0.	0.	0.
2	0.	0.	0.	0.	0.
3	0.	0.	0.	0.	0.
4	0.	0.	0.	0.	0.
5	0.	0.	0.	0.	0.
6	0.	0.	0.	0.	0.
7	0.	0.	0.	0.	0.
8	0.	0.	0.	0.	0.
9	0.	0.	0.	0.	0.
10	0.	0.	0.	0.	0.
11	0.	0.	0.	0.	0.
12	0.	0.	0.	0.	0.
13	0.	0.	0.	0.	0.
14	0.	0.	0.	0.	0.
15	0.	0.	0.	0.	0.
16	0.	0.	0.	0.	0.

ROW	COL 6	COL 7	COL 8	COL 9	COL 10
1	0.	0.	-11143771000000E+03	-.71887641000000E+02	-.33412459000000E+02
2	0.	0.	-.89921720000000E+02	-.79514879000000E+02	-.52476507000000E+02
3	0.	0.	-.62584057000000E+02	-.67133225000000E+02	-.66420909000000E+02
4	0.	0.	-.49820042000000E+02	-.51645692000000E+02	-.63545892000000E+02
5	0.	0.	-.42120167000000E+02	-.39967479000000E+02	-.47883663000000E+02
6	0.	0.	-.31447222000000E+02	-.28768635000000E+02	-.30592361000000E+02
7	0.	0.	-.19167028000000E+02	-.17237287000000E+02	-.17622054000000E+02
8	0.	0.	.14184025000000E+02	.51493748000000E+01	-.97722587000000E-01
9	0.	0.	.12314356000000E+02	.93074964000000E+01	.37888920000000E+01
10	0.	0.	.84728776000000E+01	.89586051000000E+01	.74064320000000E+01
11	0.	0.	.59769759000000E+01	.63775047000000E+01	.75132043000000E+01
12	0.	0.	.43807489000000E+01	.42023557000000E+01	.51287459000000E+01
13	0.	0.	.31919989000000E+01	.29192243000000E+01	.31082350000000E+01
14	0.	0.	.20921181000000E+01	.18761660000000E+01	.19073937000000E+01
15	0.	0.	0.	0.	0.
16	0.	0.	-.29177486000000E-01	-.25839831000000E-01	-.25236658000000E-01

TABLE 7. (CONCLUDED).

ROW	COL 11	COL 12	COL 13	COL 14	COL 15
1	-.14450086000000E+02	-.53558822000000E+01	-.17072056000000E+01	-.67829431000000E+00	0.
2	-.26740932000000E+02	-.96908041000000E+01	-.27238985000000E+01	-.93827681000000E+00	0.
3	-.49768238000000E+02	-.22729571000000E+02	-.59727675000000F+01	-.16944221000000E+01	0.
4	-.70204346000000E+02	-.48520970000000E+02	-.16366366000000E+02	-.41592302000000E+01	0.
5	-.68508736000000E+02	-.73014344000000E+02	-.41650335000000E+02	-.11777039000000E+02	0.
6	-.52278584000000E+02	-.57567293000000E+02	-.73587182000000E+02	-.36505548000000E+02	0.
7	-.22484297000000E+02	-.27341916000000E+02	-.43505294000000E+02	-.63582489000000E+02	0.
8	-.98246715000000E+00	-.42827764000000E+00	-.88615004000000E-01	-.16482048000000E-01	0.
9	.10883086000000E+00	-.58152948000000E+00	-.16238259000000F+00	-.23616125000000E-01	0.
10	.34141505000000E+01	.17932468000000E+00	-.37342153000000F+00	-.86090628000000E-01	0.
11	.67843150000000E+01	.31612987000000E+01	-.23032872000000E+00	-.29112962000000E+00	0.
12	.68914428000000E+01	.66852127000000E+01	.19595243000000E+01	-.52363704000000E+00	0.
13	.42981674000000E+01	.62151699000000E+01	.63511356000000E+01	.11045007000000E+01	0.
14	.24102347000000E+01	.29370647000000E+01	.48610779000000E+01	.56717344000000E+01	0.
15	0.	0.	0.	0.	0.
16	-.28509800000000E-01	-.44647366000000E=01	-.28186470000000E+00	-.13402537000000E+00	0.
ROW	COL 16				
1	-.42069486000000E+00				
2	-.56352512000000E+00				
3	-.96909648000000E+00				
4	-.28411344000000E+01				
5	-.14082299000000E+02				
6	-.46477438000000E+02				
7	-.30032948000000E+02				
8	-.61454346000000E-02				
9	-.74878473000000E-02				
10	-.35659495000000E-01				
11	-.28307130000000E+00				
12	-.18767190000000E+01				
13	-.53524936000000E+01				
14	-.12775815000000E+01				
15	0.				
16	-.87563367000000E+00				

TABLE 8. H<sub>2</sub> MATRIX.

ROW	COL 1	COL 2	COL 3	COL 4	COL 5
1	-53666188000000E+00	-35344084000000E+00	-15284351000000E+00	-50404551000000E-01	-76151897000000E-02
2	-41873656000000E+00	-37704808000000E+00	-24649822000000E+00	-11854559000000E+00	-33423051000000E-01
3	-28031836000000E+00	-30834058000000E+00	-30738468000000E+00	-23527058000000E+00	-10644008000000E+00
4	-21196151000000E+00	-22806121000000E+00	-28738130000000E+00	-32949708000000E+00	-23973900000000E+00
5	-16944879000000E+00	-16673957000000E+00	-20872634000000E+00	-31506689000000E+00	-36000440000000E+00
6	-11792352000000E+00	-11194623000000E+00	-12532657000000E+00	-18750317000000E+00	-27921165000000E+00
7	-69351517000000E-01	-64527993000000E-01	-69554955000000E-01	-96854443000000E-01	-13016537000000E+00
8	.54354793000000E-01	.15854806000000E-01	.63666267000000E-02	.83633876000000E-02	.37515644000000E-02
9	.45391595000000E-01	.34039208000000E-01	.11125952000000E-01	.37399917000000E-02	.51363321000000E-02
10	.29042630000000E-01	.32207012000000E-01	.26541615000000E-01	.10828201000000E-01	.19519741000000E-02
11	.18697996000000E-01	.21356696000000E-01	.26672541000000E-01	.24820806000000E-01	.11072405000000E-01
12	.12406803000000E-01	.12768691000000E-01	.17086357000000E-01	.24952065000000E-01	.25925427000000E-01
13	.81712623000000E-02	.79891329000000E-02	.94002314000000E-02	.14625664000000E-01	.23683029000000E-01
14	.49934649000000E-02	.47563187000000E-02	.53608451000000E-02	.77227810000000E-02	.10712535000000E-01
15	0.	0.	0.	0.	0.
16	-16689432000000E-03	-14287407000000E-03	-12787077000000E-03	-13568975000000E-03	-20091511000000E-03

ROW	COL 6	COL 7	COL 8	COL 9	COL 10
1	.30790430000000E-02	.25777947000000E-02	.46821622000000E+00	.12974473000000E+00	.86327743000000E-01
2	-.23303610000000E-02	.16665790000000E-02	-.28605381000000E+00	-.26497419000000E+00	-.73905082000000E-01
3	-.20269397000000E-01	-.21304467000000E-02	-.43864687000000E-01	-.16382356000000E+00	-.22068795000000E+00
4	-.75056962000000E-01	-.15018575000000E-01	.76120208000000E-01	-.58164027000000E-03	-.16353955000000E+00
5	-.20489952000000E+00	-.55783065000000E-01	.13543675000000E+00	.83965669000000E-01	-.21928415000000E-01
6	-.36331120000000E+00	-.18594837000000E+00	.15231586000000E+00	.11339847000000E+00	.54486955000000E-01
7	-.21144206600000E+00	-.32121258000000E+00	.10910357000000E+00	.85067381000000E-01	.52522437000000E-01
8	-.70582085000000E-03	-.21858512000000E-05	-.81995944000000E-01	-.63512925000000E-01	-.24785013000000E-01
9	-.15819329000000E-02	-.33999989000000E-03	-.44606124000000E-01	-.50211731000000E-01	-.35415213000000E-01
10	-.28874730000000E-02	-.89768455000000E-03	-.21252690000000F-01	-.27519346000000F-01	-.33342640000000F-01
11	-.24095458000000E-02	-.19769427000000E-02	-.17587744000000E-01	-.15893373000000E-01	-.20387880000000E-01
12	.67947050000000E-02	-.30102153000000E-02	-.16761048000000E-01	-.13028958000000E-01	-.10184110000000E-01
13	.24718244000000E-01	.38923821000000E-02	-.15211000000000E-01	-.11790686000000E-01	-.78317599000000E-02
14	.18550347000000E-01	.22646007000000E-01	-.11573093000000E-01	-.91305015000000E-02	-.64330888000000E-02
15	0.	0.	0.	0.	0.
16	-.13854846000000E-02	-.69848407000000E-03	-.10363086000000E-05	-.11183714000000E-04	-.71680059000000E-04

TABLE 8. (CONCLUDED).

ROW	COL 11	COL 12	COL 13	COL 14	COL 15
1	.10464268000000E+00	.55760488000000E-01	.16305005000000E-01	.28584274000000E-02	0.
2	.58697141000000E-01	.60257846000000E-01	.24876985000000E-01	.71799803000000E-02	0.
3	-.92135075000000E-01	.23999543000000E-01	.32706926000000E-01	.13961828000000E-01	0.
4	-.23008290000000E+00	-.10946670000000E+00	.19249782000000E-01	.21867402000000E-01	0.
5	-.19184425000000E+00	-.25884871000000E+00	-.76736371000000E-01	.19432432000000E-01	0.
6	-.27261742000000E-01	-.15209636000000E+00	-.24981268000000E+00	-.52934632000000E-01	0.
7	.17653573000000E-01	-.28779173000000E-01	-.12545484000000E+00	-.24584818000000E+00	0.
8	-.34897913000000E-02	.35592739000000E-02	.28989634000000E-02	.14122329000000E-02	0.
9	-.15935999000000E-01	-.22369098000000E-02	.18347183000000E-02	.13148627000000E-02	0.
10	-.26645343000000E-01	-.11032173000000E-01	-.81748946000000E-03	.87720969000000E-03	0.
11	-.26100727000000E-01	-.18643555000000E-01	-.60075826000000E-02	-.33529090000000E-03	0.
12	-.14650861000000E-01	-.18325944000000E-01	-.13640674000000E-01	-.35276310000000E-02	0.
13	-.54160221000000E-02	-.61406637000000E-02	-.14020059000000E-01	-.99674255000000E-02	0.
14	-.44347390000000E-02	-.22257710000000E-02	-.18766523000000E-02	-.92107446000000E-02	0.
15	0.	0.	0.	0.	0.
16	-.21263554000000E-03	-.80288678000000E-03	-.26995042000000E-02	-.11332249000000E-02	0.

ROW	COL 16
1	.20013170000000E-03
2	.28963492000000E-02
3	.77630406000000E-02
4	.15332443000000E-01
5	.11906596000000E-01
6	-.48685540000000E-01
7	-.35037781000000E-01
8	.78496212000000E-03
9	.89119628000000E-03
10	.85269406000000E-03
11	.52299105000000E-03
12	-.31773570000000E-02
13	-.15913467000000E-01
14	-.85719697000000E-02
15	0.
16	-.25164690000000E-02

TABLE 9. H<sub>3</sub> MATRIX.

ROW	COL 1	COL 2	COL 3	COL 4	COL 5
1	-.77731977000000E-02	0.	0.	0.	0.
2	0.	-.64095955000000E-02	0.	0.	0.
3	0.	0.	-.53601360000000E-02	0.	0.
4	0.	0.	0.	-.47796267000000E-02	0.
5	0.	0.	0.	0.	-.41795659000000E-02
6	0.	0.	0.	0.	0.
7	0.	0.	0.	0.	0.
9	-.46424703000000E-03	0.	0.	0.	0.
9	0.	-.34502618000000E-03	0.	0.	0.
10	0.	0.	-.25940533000000E-03	0.	0.
11	0.	0.	0.	-.20631200000000E-03	0.
12	0.	0.	0.	0.	-.15860834000000E-03
13	0.	0.	0.	0.	0.
14	0.	0.	0.	0.	0.
15	0.	0.	0.	0.	0.
16	0.	0.	0.	0.	0.

ROW	COL 6	COL 7	COL 8	COL 9	COL 10
1	0.	0.	-.46424703000000E-03	0.	0.
2	0.	0.	0.	-.34502618000000E-03	0.
3	0.	0.	0.	0.	-.25940533000000E-03
4	0.	0.	0.	0.	0.
5	0.	0.	0.	0.	0.
6	-.26170329000000E-02	0.	0.	0.	0.
7	0.	-.35266569000000E-02	0.	0.	0.
8	0.	0.	-.13126479000000E-02	0.	0.
9	0.	0.	0.	-.87929546000000E-03	0.
10	0.	0.	0.	0.	-.59438958000000E-03
11	0.	0.	0.	0.	0.
12	0.	0.	0.	0.	0.
13	-.87590870000000E-04	0.	0.	0.	0.
14	0.	-.10150294000000E-03	0.	0.	0.
15	0.	0.	0.	0.	0.
15	-.13294527000000E-04	0.	0.	0.	0.

TABLE 9. (CONCLUDED).

ROW	COL 11	COL 12	COL 13	COL 14	COL 15
1	0.	0.	0.	0.	0.
2	0.	0.	0.	0.	0.
3	0.	0.	0.	0.	0.
4	-20631200000000E-03	0.	0.	0.	0.
5	0.	-15860834000000E-03	0.	0.	0.
6	0.	0.	-87590870000000E-04	0.	0.
7	0.	0.	0.	-10150294000000E-03	0.
8	0.	0.	0.	0.	0.
9	0.	0.	0.	0.	0.
10	0.	0.	0.	0.	0.
11	-42174771000000E-03	0.	0.	0.	0.
12	0.	-28514619000000E-03	0.	0.	0.
13	0.	0.	-13880832000000E-03	0.	0.
14	0.	0.	0.	-13865191000000E-03	0.
15	0.	0.	0.	0.	0.
16	0.	0.	-56284900000000E-05	0.	0.

ROW	COL 16
1	0.
2	0.
3	0.
4	0.
5	0.
6	-46639450000000E-04
7	0.
8	0.
9	0.
10	0.
11	0.
12	0.
13	-52881158000000E-05
14	0.
15	0.
16	-13867148000000E-05

TABLE 10  
ELEMENTS OF DIAGONAL MATRIX  $F_p$

- .22960E+03  
- .25587E+03  
- .28299E+03  
- .31811E+03  
- .36114E+03  
- .41898E+03  
- .48956E+03  
- .22960E+03  
- .25587E+03  
- .28299E+03  
- .31811E+03  
- .36114E+03  
- .41898E+03  
- .48956E+03  
- .53875E+07  
- .72230E+03

TABLE 11.  $Q_R$  (m,o) STEADY STATE LIFT AND MOMENT.

ROW	COL 1	COL 2	COL 3	COL 4	COL 5
1	0.	0.	0.	0.	0.
2	0.	0.	0.	0.	0.
3	0.	0.	0.	0.	0.
4	0.	0.	0.	0.	0.
5	0.	0.	0.	0.	0.
6	0.	0.	0.	0.	0.
7	0.	0.	0.	0.	0.
8	0.	0.	0.	0.	0.
9	0.	0.	0.	0.	0.
10	0.	0.	0.	0.	0.
11	0.	0.	0.	0.	0.
12	0.	0.	0.	0.	0.
13	0.	0.	0.	0.	0.
14	0.	0.	0.	0.	0.
15	0.	0.	0.	0.	0.
16	0.	0.	0.	0.	0.

ROW	COL 6	COL 7	COL 8	COL 9	COL 10
1	0.	0.	.48535683000000E+00	.31310009000000E+00	.14552497000000E+00
2	0.	0.	.35143532000000E+00	.31076293000000E+00	.20509058000000E+00
3	0.	0.	.22114964000000E+00	.23722477000000E+00	.23470770000000E+00
4	0.	0.	.15661350000000E+00	.16235259000000E+00	.19976187000000E+00
5	0.	0.	.11663032000000E+00	.11066954000000E+00	.13258938000000E+00
6	0.	0.	.75056141000000E-01	.68663066000000E-01	.73015814000000E-01
7	0.	0.	.39151476000000E-01	.35209695000000E-01	.35995632000000E-01
8	0.	0.	-.61777233000000E-01	-.22427634000000E-01	.42562185000000E-03
9	0.	0.	-.48127411000000E-01	-.36375894000000E-01	-.14807885000000F-01
10	0.	0.	-.29940114000000E-01	-.31656501000000F-01	-.26171677000000F-01
11	0.	0.	-.18789128000000E-01	-.20048224000000E-01	-.23618391000000F-01
12	0.	0.	-.12130249000000E-01	-.11636280000000F-01	-.14201444000000E-01
13	0.	0.	-.76184509000000E-02	-.69674107000000E-02	-.74185313000000F-02
14	0.	0.	-.42734592000000E-02	-.38323452000000E-02	-.38961313000000F-02
15	0.	0.	0.	0.	0.
16	0.	0.	.40396041000000E-04	.35775116000000E-04	.34940025000000F-04

TABLE 11. (CONCLUDED).

ROW	COL 11	COL 12	COL 13	COL 14	COL 15
1	.62936035000000E-01	.23327059000000E-01	.74355791000000E-02	.29542493000000E-02	0.
2	.10450988000000E+00	.37873951000000E-01	.10645639000000E-01	.36670074000000E-02	0.
3	.17586312000000E+00	.80318161000000E-01	.21105621000000E-01	.59874807000000E-02	0.
4	.22089329000000E+00	.15252976000000E+00	.51449052000000E-01	.13074891000000E-01	0.
5	.18970000000000E+00	.20217598000000E+00	.11532936000000E+00	.32610500000000E-01	0.
6	.10090772000000E+00	.13739779000000E+00	.17563300000000E+00	.87129017000000E-01	0.
7	.45927487000000E-01	.55849888000000E-01	.88865957000000E-01	.12987659000000F+00	0.
8	.41919383000000E-02	.18653243000000E-02	.38595460000000E-03	.71786065000000E-04	0.
9	-.42533669000000E-03	.22727545000000E-02	.63462952000000E-03	.92297393000000F-04	0.
10	-.12064385000000E-01	-.63366917000000E-03	.13195379000000E-02	.30421344000000E-03	0.
11	-.21327066000000E-01	-.99378091000000E-02	.72405774000000E-03	.91519052000000E-03	0.
12	-.19082335000000E-01	-.18511286000000E-01	-.54259031000000F-02	.14499457000000E-02	0.
13	-.10258580000000E-01	-.14833955000000E-01	-.15158469000000E-01	-.26361489000000E-02	0.
14	-.49232592000000E-02	-.59993871000000E-02	-.99294673000000E-02	-.11585352000000E-01	0.
15	0.	0.	0.	0.	0.
16	.39471674000000E-04	.61814052000000E-04	.39024026000000E-03	.18555745000000E-03	0.
ROW	COL 16				
1	.18322983000000E-02				
2	.22023893000000E-02				
3	.34244398000000E-02				
4	.89313456000000E-02				
5	.38993743000000E-01				
6	.11092926000000E+00				
7	.61346718C000000E-01				
8	.26755882000000E-04				
9	.29264276000000E-04				
10	.12600788000000E-03				
11	.88985851000000E-03				
12	.51966160000000E-02				
13	.12774976000000E-01				
14	.26096482000000E-02				
15	0.				
16	.12123104000000E-02				

TABLE 12. DAMPING COEFFICIENT MATRIX D<sub>W</sub>

ROW	COL 1	COL 2	COL 3	COL 4	COL 5
1	.9423833E450974E+02	-.19431782099851E+02	.36055563170136E+01	-.33099060316053E+00	.10089201109063E+00
2	-.19431782099849E+02	.36046250709902E+02	-.17049883074519E+02	.23566430911245E+01	-.31051687170840E+00
3	.36055563170151E+01	-.17049883074519E+02	.28555311809563E+02	-.13300985477539E+02	.16967617746817E+01
4	-.33099060316027E+00	.23566430911278E+01	-.13300985477539E+02	.21418614072643E+02	-.10444000414256E+02
5	.10089201108848E+00	-.31051687170430E+00	.16967617746789E+01	-.10444000414250E+02	.1629922898708UE+02
6	-.263256824F1474E-01	.1349668620765JE-01	-.32023946243911E+00	.11363991829943E+01	-.79130558262166E+01
7	.76131453483137E-02	.20671647965206E-01	.9429985979E206E-01	-.28014580066081E-01	.10280723980426E+01
8	-.85851473218412E+00	-.23532259858794E+00	.5903576754777E-01	.11538623129301E-01	-.7899143413C000E-03
9	.28546992533727E+00	-.40954012664386E-01	-.1878805P709037E+00	.74797199836286E-01	-.11384625C32611E-01
10	-.5410013F406241E-01	.199818385F7123E+00	-.11366847211329E-01	-.11388749622210E+00	.28192028619248E-01
11	.72165154919545E-02	-.23554660323266E-01	.14147789939609E+00	.4909253359373E-01	-.15014444205685E+00
12	-.51015019697292F-13	.8381184944E601F-02	-.29507648510172E-01	.12919695575782E+00	-.47945459183341E-01
13	-.16075159286277E-02	-.96902917834391E-02	-.71562412504158E-02	-.438640320356767E-01	.12922653243488E+00
14	.88605382903561E-02	.3475868794819E-01	.5106354473423FE-01	.31157577162947E-01	-.32421437557078E-01
15	-.13389798469420E-03	.18271507426827E-03	-.15886362136006E-02	.50528290852892E-02	-.2268691050E055E-01
16	-.163979628L0696E-01	-.40411051328436E-01	-.60235207769070E-01	-.32940443848187E-01	.175446625L486E-01

ROW	COL 6	COL 7	COL 8	COL 9	COL 10
1	-.263256824E1683E-01	.75131453483362E-02	-.85851473218393E+00	.28546992533707E+00	-.54190138406084E-01
2	.13496686204253E-01	.20671647965129E-01	-.23532259858743E+00	-.40954012663854E-01	.199818385E7208E+00
3	-.32023946244124E+00	.94899859784848E-01	.59035767548266E-01	-.1878805P708943E+00	-.11306840209494E-01
4	.1136399182913E+01	-.28014580065410E-01	.11538623129721F-01	.74797199837067E-01	-.11388749622063E+00
5	-.7913058262173E+01	.1028072308U414E+01	-.78991434096417E-03	-.11384625032704E-01	.28192028619716E-01
6	.12013110047109E+02	-.4729149U201940E+01	-.15614183276863E-01	-.362452432048447E-01	-.43739299520445E-01
7	-.47291490201949E+01	.37457446772104E+01	.2374456A173P5PE-02	.58960625876709E-02	.89897E99484620E-02
8	-.15614183276894E-01	.2374456175321E-02	.78641236R2505E+00	-.85329937635725E-01	-.67360427945353E-02
9	-.36245243204844E-01	.58960625879123E-02	-.85329937635720F-01	.35613731413008E+00	-.759784844L6561E-01
10	-.43739299519895E-01	.898978944888E-02	-.673604279458C3E-02	-.75978484400637E-01	.26540564220142E+00
11	-.20342631612942E-02	.10021353165841E-01	.12800587052473F-02	-.33052377567463E-02	-.50995072999878E-01
12	-.82354668737481E-01	.33555064798169E-01	.46473404603712E-03	.6162140194867E-04	-.56867103577421E-02
13	-.49434949637129E-01	-.26830536561611E-01	-.19992966871740E-02	-.52155116925262E-02	-.70698451566798E-02
14	.24725026687474E-01	-.66787638206815E-01	.7586213018P14E-02	.17796527109582E-01	.18684761782671E-01
15	-.4470951437593E-02	.23450319359180E-01	-.40774656893779E-04	-.9544C48531657E-04	-.15009647514422E-03
16	.70023036844029E-01	-.43060800757901E-02	-.92304165342501E-02	-.21990114318806E-01	-.243674827764L-01

TABLE 12. (CONCLUDED).

ROW	COL 11	COL 12	COL 13	COL 14	COL 15
1	.72165154921889E-02	-.51015019609527E-03	-.16075159283304E-02	.P8606382915156E-02	-.13389798473057E-03
2	-.23554660322498E-01	.83811849044367E-02	-.96902917833216E-02	.34758068794712E-01	.18271507417354E-03
3	.14147769930709F+00	-.29507648509549E-01	-.71562412503540E-02	.51063844734048E-01	-.15886302136499E-02
4	.49092533060423E-L1	.12919695575850E+00	-.43840320356645E-01	.31157577164291E-01	.50528290852995E-02
5	-.15014444205687E+00	-.47945459183516E-01	.12922853743453E+00	-.32421437596773E-01	-.22668910568057E-01
6	-.20342631823440F-02	-.82354668738224E-01	-.49434949637167E-01	.24725026669194E-01	-.44709551437553E-02
7	.10021353165815E-01	.33555064798053E-01	-.26830536561513E-01	-.66787638207101E-01	.23450319359185E-01
8	.12800587053105E-02	.46473404616781E-03	-.19992986870627E-02	.75886213018616E-02	-.40774656598314E-04
9	-.33052377566275F-02	.61621402075285E-04	-.521551189924057E-02	.17796527109118E-01	-.95044048527632E-04
10	-.5099507299982F-01	-.56867103575809E-02	-.70698451567069E-02	.16884761782180E-01	-.15009647514242E-03
11	.19024207472722E+00	-.42254050066570E-01	-.11746148396294E-01	.12530707161885E-01	-.71496425835160E-04
12	-.4225496066653E-L1	.12739492210793E+00	-.33029917366229E-01	-.21795664862644E-02	.70245241918291E-03
13	-.11746148396445E-L1	-.33029917366326E-01	.12322767839431E+00	-.36827653466936E-01	-.14074129495596E-01
14	.12530707162479F-01	-.21795664869204E-02	-.36827653466936E-01	.11388843681788E+00	-.40534804613113E-02
15	-.71496425837200F-04	-.70245241918493E-03	-.14074129495897E-01	-.40534804613084E-02	.14554562670986E-01
16	-.19246646151151E-L1	-.67042999383535E-02	.59525227153711E-02	-.33800440410569E-01	.10171284394534E-03
ROW	COL 16				
1	-.10397962800692E-01				
2	-.40411051329170E-01				
3	-.60235207764203E-L1				
4	-.32940443849552E-01				
5	.17544662505932E-L1				
6	.70023036844657E-01				
7	-.43060007560111E-L2				
8	-.92304166341862E-02				
9	-.21990114318594E-01				
10	-.24367408277302E-01				
11	-.19246646150750E-01				
12	-.67042999380236F-C2				
13	.59525227155444E-L2				
14	-.3380044041004E-L1				
15	.10171284394677F-03				
16	.39305978978055E-L1				









TABLE 13. (CONCLUDED).

0.	0.	0.
0.	0.	0.
0.	0.	0.
0.	0.	0.
0.	0.	0.
0.	0.	0.
0.	0.	0.
0.	0.	0.
0.	0.	0.
0.	0.	0.
0.	0.	0.
0.	0.	0.
0.	0.	0.
0.	0.	0.
0.	0.	0.
0.	0.	0.
0.	0.	0.
0.	0.	0.
0.	0.	0.
0.	0.	0.
0.	0.	0.
.5527E+06	.4458E+04	0.
.7944E+06	.6409E+04	0.
.8484E+06	.6844E+04	0.
.9335E+06	.7531E+04	0.
.1034E+07	.8344E+04	0.
.8570E+06	.6913E+04	0.
.5503E+06	.4439E+04	0.
-.1899E+07	-.1524E+05	0.
-.4039E+07	-.3258E+05	0.
-.5415E+07	-.4369E+05	0.
-.6254E+07	-.5045E+05	0.
-.7249E+07	-.5848E+05	0.
-.4873E+07	-.3931E+05	0.
-.2203E+07	-.1777E+05	0.
0.	0.	-.7582E+05
.2009E+08	.1621E+06	.9000E+05
-.3419E+04	-.2758E+02	0.
-.3693E+04	-.2984E+02	0.
-.3143E+04	-.2535E+02	0.
-.3172E+04	-.2559E+02	0.
-.3173E+04	-.2560E+02	0.
-.2753E+04	-.2221E+02	-.4198E+01
-.1717E+04	-.1385E+02	0.
.2223E+04	.1793E+02	0.
.3277E+04	.2643E+02	0.
.2999E+04	.2420E+02	0.
.2445E+04	.1972E+02	0.
.1903E+04	.1535E+02	0.
.4951E+03	.3994E+01	-.4759E+00
.2495E+03	.2013E+01	0.
0.	0.	0.
-.1183E+02	-.9543E-01	-.1248E+00
0.	.1000F+01	0.
-.3773E+05	-.6088E+03	0.
0.	0.	-.2140E+03

TABLE 14. REAL JORDAN EIGEN VALUE MATRIX ( $\Omega$ )<sub>51x51</sub>

$\alpha_i$	$w_i$		
-53874636E+07	0	-36575524E+02	.66329116E+03
-70628296E+03	0	-36575524E+02	-.66329116E+03
-53874636E+03	0	-34603439E+02	.77577360E+03
-42650037E+03	0	-34603439E+02	-.77577360E+03
-42076832E+03	0	-39687059E+02	.82053953E+03
-37941934E+03	0	-39687059E+02	-.82053953E+03
-36448804E+03	0	-59058862E+02	.90825432E+03
-33232312E+03	0	-59058862E+02	-.90825432E+03
-32098716E+03	0	-15792003E+02	.12784471E+04
-29445312E+03	0	-15792003E+02	-.12784471E+04
-28404553E+03	0	-17795688E+02	.18628329E+04
-26623081E+03	0	-17795688E+02	-.18628329E+04
-25450833E+03	0	-20832288E+02	.26384182E+04
-23248749E+03	0	-20832288E+02	-.26384182E+04
-22823720E+03	0	-28390006E+02	.56179762E+04
-214000000E+03	0	-28390006E+02	-.56179762E+04
-70037027E+02	0		
-10819853E+02	.59806279E+02		
-10819853E+02	-.59806279E+02		
-40011849E+02	.78504192E+02		
-40011849E+02	-.78504192E+02		
-58556715E+01	.16229324E+03		
-58556715E+01	-.16229324E+03		
-39947712E+02	.22547021E+03		
-39947712E+02	-.22547021E+03		
-12505607E+03	.35231884E+03		
-12505607E+03	-.35231884E+03		
-26405194E+02	.37729018E+03		
-26405194E+02	-.37729018E+03		
-16578781E+02	.41824391E+03		
-16578781E+02	-.41824391E+03		
-50170125E+03	.23233139E+01		
-50170125E+03	-.23233139E+01		
-37455522E+02	.55769308E+03		
-37455522E+02	-.55769308E+03		

## REFERENCES

1. Abel, I., "An Analytic Technique for Predicting the Characteristics of a Flexible Wing Equipped With an Active Flutter Suppression System and Compared With Wind Tunnel Data," NASA TN 1367, 1979.
2. Gangsaas, D., and Ly, U., "Application of a Modified Linear Quadratic Gausson Design to Active Control of a Transport Airplane," A.I.A.A. Conference on Guidance and Control, Aug. 6-8, 1979, Boulder, Col.
3. Nissim, E., and Abel, I., "Development and Application of an Optimization Procedure for Flutter Suppression Using the Aerodynamic Energy Concept," NASA TP 1137, Feb., 1978.
4. Edwards, J. W., Breakwell, J. V., Bryson, A. E., "Active Flutter Control Using Generalized Unsteady Aerodynamic Theory," J.G.C., Vol. 1, No. 1, Jan. - Feb., 1978.
5. Creedon, J., "Control of the Optical Surface of a Thin, Deformable Primary Mirror with Application to an Orbitory Astronomical Observatory," Automatica, Vol. 6, pp. 643-660, 1970.
6. Ostroff, A. J., "Evaluation of Control Laws and Actuator Locations for Control Systems Application to Deformable Astronomical Telescope Mirror," NASA TN D-7276, Oct. 1973.
7. Edwards, J. W., "Unsteady Aerodynamic Modeling and Active Aeroelastic Control," NASA - CR - 148019, Feb., 1977.
8. Morino, L., "Steady, Oscillatory and Unsteady Subsonic and Supersonic Aerodynamics - Vol. I, Theoretical Manual," NASA - CR - 159130, Jan., 1980.
9. Scott, A. S., Pruens, R. D., Tseug, K., Morino, L., "Steady, Oscillatory and Unsteady Subsonic and Supersonic Aerodynamics - Vol. II - User's Manual," NASA CR 159131, June 1980.
10. Albano, E., Roddes , W. P., "A Doublet Lattice Method for Calculating Light Distributions on Oscillating Surfaces in Subsonic Flows," A.I.A.A.J., Vol. 7, No. 2, Feb., 1969.
11. Vepa, R., "On the Use of Pade' Approximants to Represent Unsteady Aerodynamic Loads for Arbitrary Small Motions of Wings," A.I.A.A. 14th Aerospace Science Meeting, Washington, D. C., Jan. 26, 1976.
12. Edwards, J. W., "Applications of Laplace Transform Methods to Airfoil Motion and Stability Calculations," 20th Structural Dynamics and Materials Conference, April 1979, St. Louis, Missouri.
13. Roger, K. L., "Airplane Math Modeling for Active Control Design," AGARD-CP-228, Aug. 1977, pp. 4-1/11.

1. Report No. NASA CR-166023	2. Government Accession No.	3. Recipient's Catalog No.	
4. Title and Subtitle  ANALYTICAL PROCEDURES FOR FLUTTER MODEL DEVELOPMENT AND CHECKOUT IN PREPARATION FOR WIND TUNNEL TESTING OF THE DAST ARW-1 WING		5. Report Date December 1982	
7 Author(s)  Samuel Pines		6. Performing Organization Code	
9 Performing Organization Name and Address  Analytical Mechanics Associates, Inc. 17 Research Road Hampton, Virginia 23666		8. Performing Organization Report No. AMA 82-35	
12. Sponsoring Agency Name and Address  National Aeronautics and Space Administration Washington, D. C. 20546		10. Work Unit No.	
		11. Contract or Grant No. NAS1-15593	
		13. Type of Report and Period Covered Contractor Report	
		14. Sponsoring Agency Code	
15. Supplementary Notes  Langley Technical Monitor: Aaron J. Ostroff			
16. Abstract  This report contains the results of a study to develop analytical procedures to be used in the checkout and calibration of flutter wind tunnel model of the DAST ARW-1 wing equipped with a flutter suppression device. The report contains a description of the methods used to obtain a realistic simulation of the structural inertial and aerodynamic properties of the wing, the hydro-electro-servo actuator used for flutter suppression, a prediction of the open loop flutter speed at a fixed Mach number (.897), a procedure for checkout and calibration using the method frequency response of a wing mounted accelerometer, and an analytical representation of a reduced state approximation of the overall system.			
17 Key Words (Suggested by Author(s))  Flutter suppression, control theory, Padé approximates, state reduction, hydraulic-electro-servo simulation		18. Distribution Statement  Unclassified - Unlimited	
19. Security Classif. (of this report) Unclassified	20. Security Classif. (of this page) Unclassified	21. No. of Pages 81	22. Price